Phil. Trans. R. Soc. Lond. A **326**, 117–150 (1988) [117]
Printed in Great Britain

Collision tectonics of the Ladakh–Zanskar Himalaya

By M. P. Searle, D. J. W. Cooper and A. J. Rex
*Department of Geology, University of Leicester, Leicester LE*1 *7RH, U.K.*

[Plates 1–4]

The collision of the Indian Plate with the Karakoram–Lhasa Blocks and the closing of Neo-Tethys along the Indus Suture Zone (ISZ) is well constrained by sedimentologic, structural and palaeomagnetic data at *ca.* 50 Ma. Pre-collision high *P*–low *T* blueschist facies metamorphism in the ISZ is related to subduction of Tethyan oceanic crust northwards beneath the Jurassic–early Cretaceous Dras island arc. The Spontang ophiolite was obducted southwestwards onto the Zanskar shelf before the Eocene closure (D1). The youngest marine sediments on the Zanskar shelf and along the ISZ are Lower Eocene, after which continental molasse deposition occurred.

After ocean closure, thrusting followed a SW-directed piggy-back sequence (D2). This has been modified by late-stage breakback thrusts, overturned thrusts and extensional normal faulting associated with culmination collapse and underplating. The ISZ and northern Zanskar shelf sequence are affected by late Tertiary N-directed backthrusting (D3), which also affects the Indus molasse. A 50 km wide 'pop-up' zone with divergent thrust vergence was developed across the Zanskar Range. Balanced and restored cross sections indicate a minimum of 150 km of shortening across the Zanskar shelf and ISZ.

Post-collision crustal thickening by thrust stacking resulted in widespread Barrovian metamorphism in the High Himalaya that reached a thermal climax during Oligocene–Miocene times. Garnet–biotite–muscovite ± tourmaline granites were generated by intracrustal partial melting during the Miocene within the Central Crystalline Complex. Their emplacement on the hangingwall of localized ductile shear zones was associated with SW-directed thrusting along the Main Central Thrust (MCT) zone and concomitant culmination collapse normal faulting along the Zanskar Shear Zone (ZSZ) at the top of the slab. Metamorphic isograds have become inverted by post-metamorphic SW-verging recumbent folding and thrusting along the base of the High Himalayan slab. Along the top of the slab, isograds are the right way up but are structurally and thermally telescoped by normal faulting along the ZSZ.

1. Introduction

It is now widely accepted that the collision between the Indian Plate and the collage of previously sutured micro-continental plates of Central Asia occurred during the mid- to late Eocene, at approximately 50–45 Ma (see, for example, Allègre *et al.* 1984; Searle *et al.* 1987). The timing of terminal collision of the two plates is deduced from (i) the ending of marine sedimentation in the Indus Suture Zone (ISZ), (ii) the beginning of continental molasse sedimentation along the suture zone, (iii) the ending of Andean-type calc-alkaline magmatism along the Trans-Himalayan (Ladakh–Kohistan–Gangdese) batholith and (iv) the initiation of the major collision-related thrust systems in the Himalayan Ranges.

Palaeomagnetic data indicate that over 2000–2500 km of southern (Neo-) Tethys separated the Indian and Central Asian Plates during the late Cretaceous, with initial collision at about 55 Ma (Klootwijk 1979) and terminal collision at about 40 Ma (Molnar & Tapponnier 1975; Klootwijk & Radhakrishnamurthy 1981). The northward relative motion of the Indian Plate decreased threefold at 40 Ma from average rates of 14.9 ± 4.5 cm a^{-1} to 5.2 ± 0.8 cm a^{-1} (Pierce 1978). Seafloor spreading rates in the Indian Ocean also decreased drastically at anomaly 22, which corresponds in time to *ca.* 50 Ma (Sclater & Fisher 1974; Johnson *et al.* 1976). Major directional shifts in the relative motion of the Indian Plate at anomalies 22 and 21 (50–48 Ma) are also thought to indicate the onset of collision (Patriat & Achache 1984). Another major shift occurred at anomaly 13 (36 Ma) after which India resumed stable northwards convergence with a constant rate of 5 cm a^{-1} (Patriat & Achache 1984).

The post-collision crustal shortening in the Indian Plate can only be deduced from the restoration of balanced cross sections across the Himalaya. It is widely recognized that in

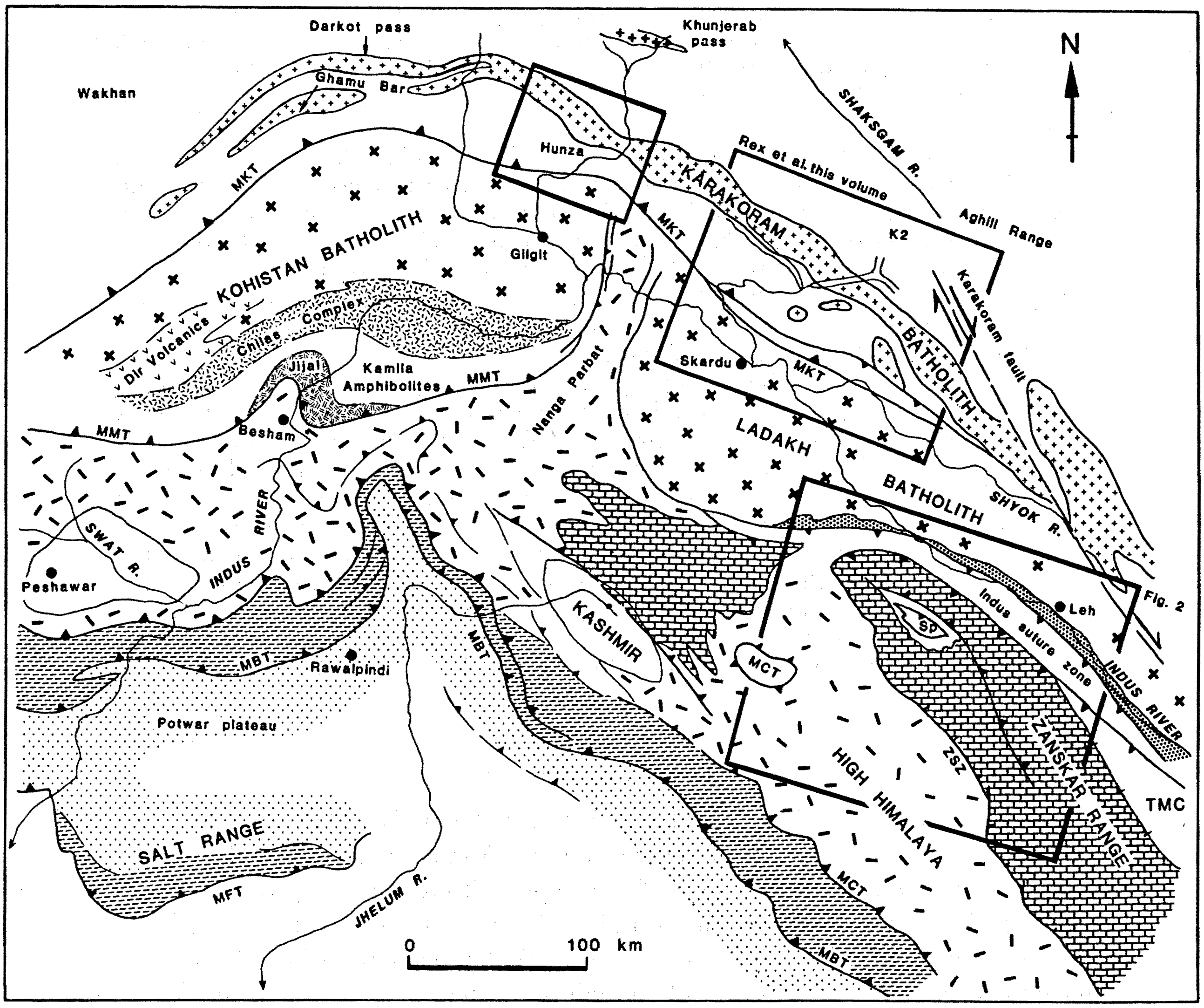

FIGURE 1. Geological sketch map of the western Himalaya–Karakoram showing the Ladakh–Zanskar Himalaya in box and central Karakoram described in the accompanying paper (Rex *et al.* this symposium). Abbreviations: MKT, Main Karakoram Thrust; MMT, Main Mantle Thrust; MCT, Main Central Thrust; MBT, Main Boundary Thrust; MFT, Main Frontal Thrust; Sp, Spontang ophiolite.

general terms, southward-propagating thrust stacking had occurred across the Himalaya since the mid-Eocene collision and suturing (see, for example, Molnar 1984; Mattauer 1986; Searle *et al.* 1987).

The climax of crustal shortening and thrust stacking occurred during the mid-Tertiary in the High Himalaya and Zanskar Ranges, with thrusts propagating southwestwards from the Main Central Thrust (MCT) system to the Lesser Himalaya and the late Tertiary Main Boundary Thrust (MBT) system (figure 1). The youngest thrusts occur along the southern boundary of the Himalaya, in the Siwalik molasse deposits of the Indian foreland basin, where the Main Frontal Thrust (MFT) terminates at tip lines below the Indo–Gangetic plains.

Four major tectonic zones constitute the Ladakh–Zanskar Himalaya. These are, from north to south, the Ladakh (Transhimalayan) batholith, the Indus Suture Zone, the Tibetan-Tethys (Zanskar shelf) Zone, and the High Himalaya. A generalized geological map depicting these

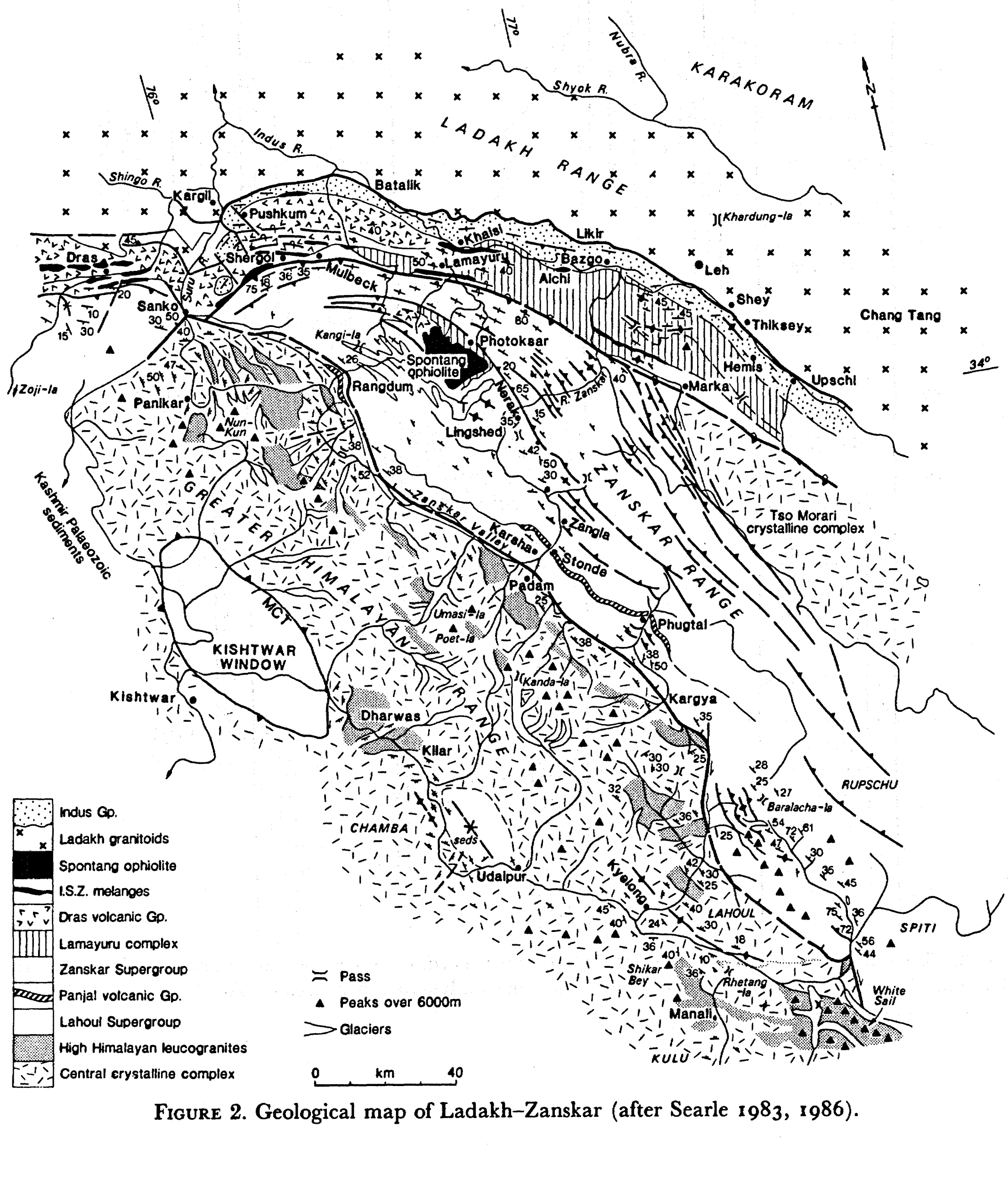

FIGURE 2. Geological map of Ladakh–Zanskar (after Searle 1983, 1986).

zones is shown in figure 2. This paper reviews and summarizes the geology of these four zones in the western Himalaya and discusses the timing of deformation, the mechanism of crustal thickening, the amounts of crustal shortening and models for collision tectonics in the Himalaya. Figure 3 shows a late Cretaceous and Tertiary time chart for the Ladakh–Zanskar Himalaya (after Searle 1983, 1986) updated with all radiometric ages and stratigraphic time spans for the four tectonic zones.

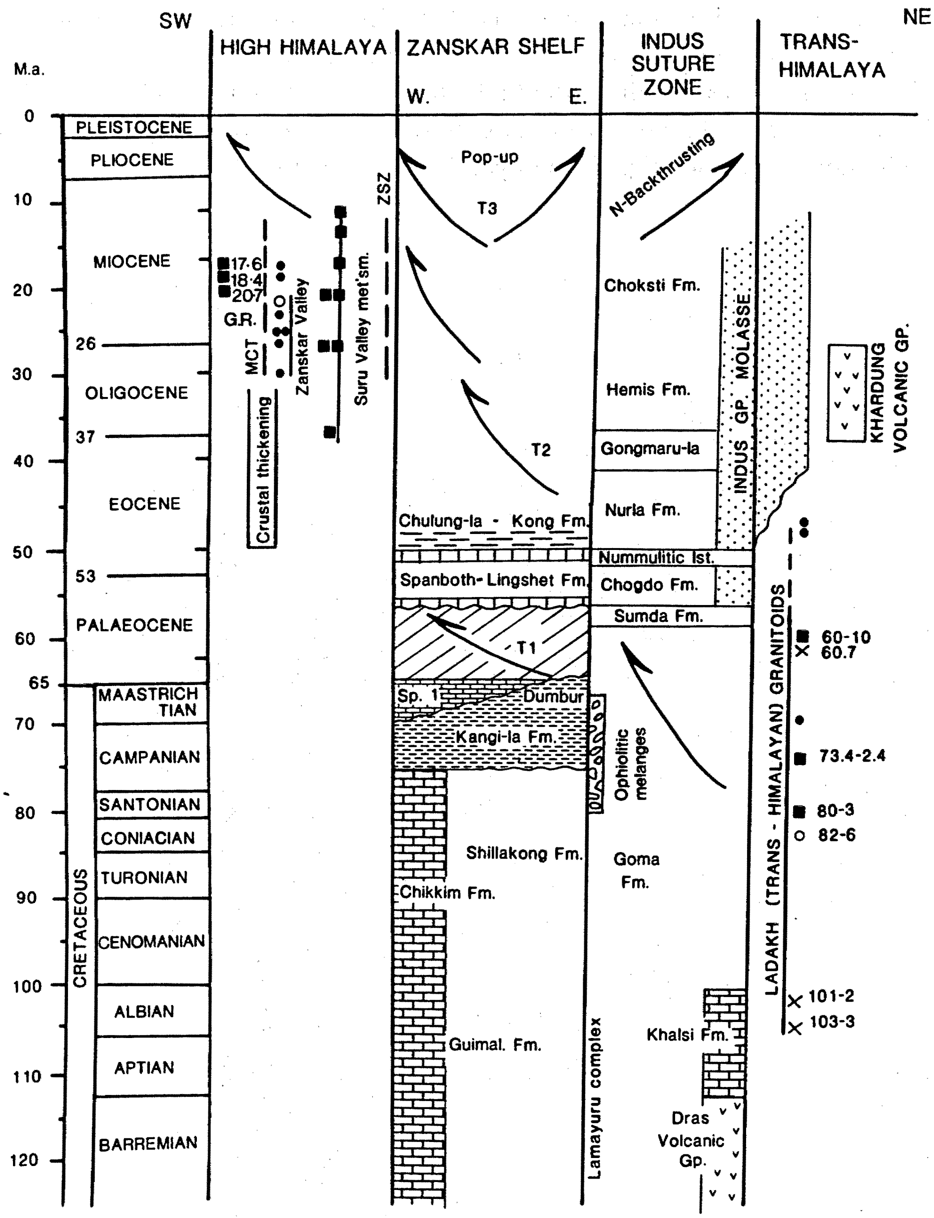

FIGURE 3. Revised time chart for the late Cretaceous–Tertiary rocks of the four tectonic zones in the Ladakh–Zanskar Himalaya. Crosses, U–Pb ages; squares, Rb–Sr; open circles, ^{39}Ar–^{40}Ar; dots, K-Ar. See text for sources of data and discussion.

2. Structural framework

Searle (1983, 1986) defined three major stages of deformation in the Western Himalaya: (1) a pre-collision ophiolite obduction phase (T1: 75–60 Ma), (2) a continental collision stage (T2: 45–25 Ma) and (3) a post-collision stage (T3: 15–0 Ma). The timing of motion on thrusts was determined by combining detailed structural mapping with stratigraphy and fault geometry (folded thrusts, truncated folds, truncated thrusts, etc.). In the High Himalaya, offsets were estimated by determining the differences in P–T conditions in the footwall and hangingwall of shear zones.

Determination of the sequence of thrusting is critical to the understanding of the geology of Ladakh–Zanskar. Therefore it is necessary at this point to define four major types of thrusts. Piggy-back thrusts propagate in-sequence towards the foreland (India) and preserve intact stratigraphy in the footwall. They cut up-section in the transport direction and place older rocks over younger (see Butler (1987) for a review). Out-of-sequence thrusts develop in the hangingwall of earlier thrusts and may eliminate some stratigraphic section in the footwall. They may truncate folds and thrusts in the footwall and place younger rocks on to older. Breaching thrusts are thrusts that cut through the roof thrust of a duplex and may cause small-scale reversals of stacking order. Breakback thrusts cut through a previously assembled stack of thrust sheets and place originally lower, younger thrust sheets over originally higher, older thrust sheets. They may truncate earlier folds and thrusts in the footwall and therefore cross sections must be sequentially restored in a reverse time sequence.

3. Ladakh batholith

The Ladakh batholith, a part of the 2000 km long Transhimalayan batholith, is situated to the north of the ISZ in the Ladakh Ranges (figure 2). The Transhimalaya belt continues westward to include the Kohistan batholith in northern Pakistan (Petterson & Windley 1985) and eastward to include the Gangdese batholith in south Tibet (Allègre *et al.* 1984; Tapponnier *et al.* 1981). The Ladakh batholith ranges in composition from olivine–norite to leucogranites with grandiorites dominating (Thakur 1981; Honegger *et al.* 1982). Olivine–orthopyroxene-bearing norites, gabbros, diorites, granodiorites, granites and leucogranites are all represented and collectively represent a continental, subduction-related batholith (Honegger *et al.* 1982). The presence of granitic gneisses and metasedimentary sequences in the Ladakh Range provides evidence for the existence of precursory continental crust (Honegger & Raz 1985). Furthermore, a substantial component of inherited lead in zircons extracted from samples of the batholith implies involvement of continental crust during petrogenesis (Schärer *et al.* 1984). Initial $^{87}Sr/^{86}Sr$ ratios of around 0.704 (Schärer *et al.* 1984) and 0.705 (Honegger *et al.* 1982) are unenriched, inferring a primary mantle derivation of the magmas. The amount of isotopic enrichment due to the envisaged crustal component remains to be quantified.

Available geochronological determinations indicate that the Ladakh batholith is composite and dominated by pre-collisional magmatic events. U–Pb zircon ages of 103 ± 3 Ma (Honegger *et al.* 1982) and 101 ± 2 Ma (Schärer *et al.* 1984) from samples collected near Kargil refer to important mid-Cretaceous magmatism. A second U–Pb determination of monazite/allanite from a biotite–granite near Leh gave an age of 60.7 ± 0.4 Ma, whereas a Rb–Sr isochron age of 73 ± 2.4 Ma (Schärer *et al.* 1984) and a $^{39}Ar/^{40}Ar$ age of 82 ± 6 Ma (Schärer & Allègre 1982) may indicate a continuity of magmatic activity for some 40 Ma, finally terminating with continent–continent collision (figure 3). However, the latter two age determinations may also be interpreted as cooling events on the argument that these isotopic systems have lower blocking temperatures (Schärer *et al.* 1984). Likewise, a span of K–Ar mineral ages of 50–40 Ma is considered to reflect a cooling period associated with uplift.

The termination of granitic magmatism in the Ladakh batholith is contemporaneous with the closing of Neo-Tethys along the ISZ and the change from marine to continental sedimentation. Clasts of granites, andesites and rhyolites are particularly widespread in the conglomerates of the Chogdo, Nurla and Hemis Formations of the Indus Group molasse, which unconformably overlies the batholith. Volcanic rocks overlying the Ladakh batholith include andesites and rhyolites (Srimal *et al.* 1987). Late-stage garnet–muscovite leucogranitic dykes intrude the granite and may reflect a final phase of intracrustal melting after the 50 Ma collision along the ISZ.

Granitoids of the Ladakh batholith intrude the Dras island arc volcanics and rocks of the suture zone around Kargil. This provides strong evidence that the Dras island arc was accreted to the Karakoram–Lhasa Blocks by the mid-Cretaceous and that the Shyok (Northern) Suture between the Ladakh and Karakoram terranes closed in the mid-Cretaceous (Coward *et al.* 1986; Pudsey 1986; Searle *et al.* 1988) and not in the late Tertiary (Thakur 1981, 1987).

The Ladakh batholith has undergone an unknown amount of post-collision shortening evidenced by thrusting within the granitoids. Near Kargil, a number of late stage shear zones with mylonitized amphibolites and greenschists cut intrusive rocks of the batholith.

4. Indus Suture Zone

The Indus Suture Zone (ISZ) defines the zone of the collision between the Indian Plate and the Karakoram–Lhasa Block to the north (Gansser 1964, 1977; Allègre *et al.* 1984; Searle *et al.* 1987) and can be traced for over 2000 km from Kohistan and Ladakh in the east right across southern Tibet to the NE Frontier region of India–Burma. In Tibet it is commonly referred to as the Yarlung–Tsangpo Suture; in the western Himalaya it is the Indus Suture Zone. To the west of Ladakh, the ISZ is folded around the giant Nanga Parbat fold, a 35 km wavelength, upright anticlinorium that exposes Indian Plate gneisses equivalent to the Central Crystalline Complex in its core (figure 1). The ISZ has been offset by the late Tertiary culmination of Nanga Parbat and downfaulted west of Nanga Parbat along the Rakhiot Fault zone. It continues westwards as the Main Mantle Thrust (MMT) across southern Kohistan (Tahirkheli & Jan 1979).

In Ladakh, the Indus Suture is bounded to the south by the backthrust shelf sediments of the Zanskar Supergroup and the Tso Morari crystalline complex, and to the north by the Ladakh batholith. The geology of the ISZ has been described by Gupta & Kumar (1975), Shah *et al.* (1976), Andrieux *et al.* (1981), Fuchs (1977, 1979), Bassoullet *et al.* (1978, 1981), Frank *et al.* (1977), Baud *et al.* (1982), Brookfield & Andrews-Speed (1984*a*, *b*), Thakur (1981, 1987) and Searle (1983, 1986).

The Indus Suture Zone in Ladakh consists essentially of three major linear thrust belts, the Lamayuru complex, the Nindam–Dras Volcanic Group and the Indus Group molasse. They are separated by major fault zones or ophiolitic melange belts (figure 7*a*, plate 1). Figure 4 is a palaeogeographic reconstruction of the Neo-Tethyan basin showing the pre-Eocene stratigraphy of the rocks now preserved in the ISZ in Ladakh.

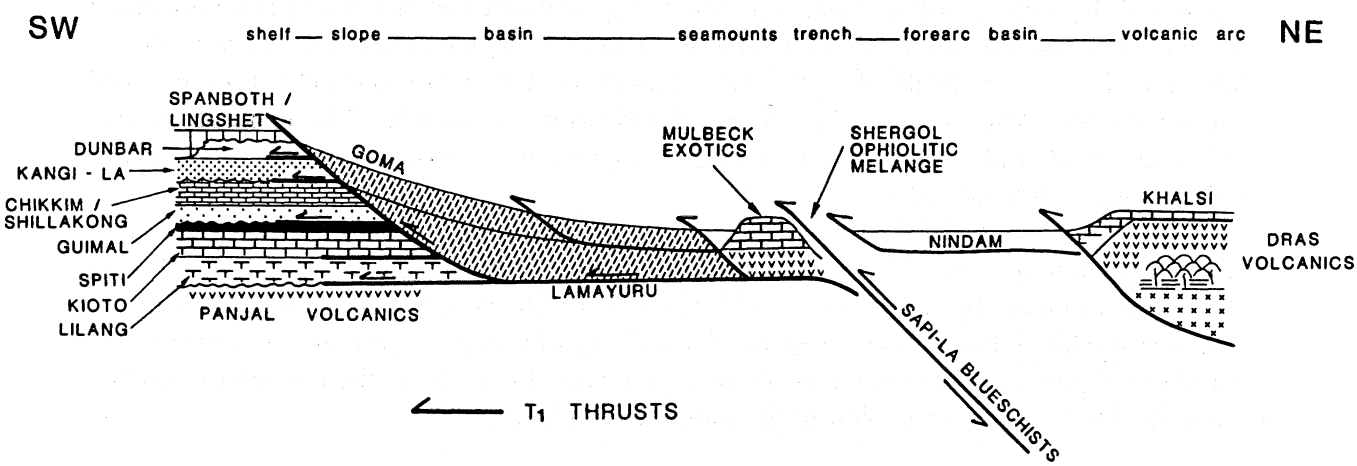

FIGURE 4. Palaeogeographic reconstruction of the Ladakh Tethys showing stratigraphic units along the Indus Suture Zone in Ladakh.

(a) *Lamayuru complex*

This complex is the passive-margin deep-water sediments, consisting mainly of shales with indurated sandstones and limestones, that show evidence of distal turbidity current deposition (Frank *et al.* 1977; Fuchs 1977, 1979, 1982). The Lamayuru complex rocks are now preserved as a series of SW-dipping inverted imbricate slices, the early SW-directed thrusts having been rotated during the late Tertiary phase of N-directed backthrusting. In the Indus Suture Zone the Lamayuru complex has been dated at late Triassic to (?)mid-Jurassic (Fuchs 1977; Bassoullet *et al.* 1981). The highest preserved stratigraphic units are thick-bedded limestone conglomerates and oolitic grainstones that crop out as dismembered sheets between Prinkiti-la (Lamayuru gompa) and the Namika-la east of Mulbeck (figure 2), and record a period of platform margin collapse.

On the Zanskar shelf, a sequence of slates of possible Cretaceous age (Goma Formation) (Colchen *et al.* 1986) crops out in a thrust slice beneath the Spontang ophiolite. These rocks are part of the Lamayuru complex (Bassoullet *et al.* 1978, 1981) and were emplaced along with the overlying Dras volcanic, Spontang ophiolite and mélange units onto the Zanskar shelf from the Indus Suture before ocean closure.

(b) *Ophiolitic mélanges*

Narrow zones of ophiolitic mélange bound both northern and southern margins of the Dras volcanic and Lamayuru complex rocks along the ISZ. The widest zone separates the Lamayuru complex from the Nindam Formation–Dras Volcanic Group (the Shergol ophiolitic mélange of Thakur (1981) and Searle (1983)). Blocks consist of MORB–tholeiitic basalts, alkali basalts and amygdaloidal pillow lavas, agglomerates, gabbros, rodingites, dunites, harzburgites, radiolarian cherts and deep-sea sediments.

Pelagic limestones intercalated within the mélange in the Mulbeck–Pushkum area (figure 2) have yielded Campanian–Maastrichtian Foraminifera (Colchen *et al.* 1986). The late Cretaceous age of the ophiolitic mélange corresponds to the proposed timing of obduction of the Spontang ophiolite on to the Zanskar shelf (Searle (1986, 1987; see also following section).

Around the Sapi-la, SW of Shergol (figure 2), a prominent belt of blueschists is imbricated within the mélange and overlain by Oligocene–Miocene conglomerates of the molasse (figure 7*b*, plate 1). Around Mulbeck a few large olistoliths of Permian and later Triassic reefal limestones (the Mulbeck exotics) are associated with uncommon Triassic alkali basalts (Honegger *et al.* 1982; Searle 1983), thought to be related to oceanic island (within-plate) volcanic seamounts in Tethys.

A large number of E–W striking serpentinite shear zones cut the suture zone rocks and frequently contain greenschists and crossite or glaucophane-bearing blueschists. One of these shear zones bounds the northern margin of the Dras Volcanic Group along a N-directed backthrust with Indus molasse along the footwall (Searle 1983) (figure 6*e*), well exposed at Pushkum (figure 2). A lenticular serpentinite shear zone also separates the Lamayuru complex from the Zanskar shelf succession to the south of Lamayuru.

(*c*) *Dras Volcanic Group*

A thick sequence of clinopyroxene, hornblende and plagioclase–phyric basalts, andesites and dacites together with intercalated volcaniclastics and minor amounts of tholeiitic pillow lavas make up the Dras Volcanic Group in western Ladakh (Wadia 1937; Thakur 1981; Honegger *et al.* 1982; Searle 1983). They represent the lateral equivalents to the Chalt volcanics in the upper part of the Kohistan island arc sequence in Pakistan (Coward *et al.* 1986), but are not present anywhere along the ISZ east of Ladakh. Uncommon radiolarian cherts interbedded in the Dras volcanic rocks west of Dras (figure 2) have yielded Callovian–Tithonian ages (Honegger *et al.* 1982). In central Ladakh, *Orbitolina*-bearing limestones of Albian–Aptian age (Khalsi limestone, figure 4) stratigraphically overlie the Dras volcanic rocks.

Basalts of the Dras Volcanic Group are enriched in K, Ba, Rb, Sr and the light rare earth elements (LREES) and depleted in the high field strength (HFS) elements Ti, Zr, Y, Nb and the HREES relative to MORB (Honegger *et al.* 1982; Dietrich *et al.* 1983; Radhakrishna *et al.* 1984). Their geochemical signature may be compared with modern-day island-arc tholeiites and primitive calc-alkaline volcanic rocks (Pearce & Cann 1973).

Around Kargil, olivine–orthopyroxene-bearing gabbro–norites may represent relic magma chamber cumulates associated with the Dras volcanics. They are similar to the volumetrically abundant granulite–facies rocks of the Chilas complex at the base of the Kohistan island arc in Pakistan (Tahirkheli & Jan 1979; Coward *et al.* 1986).

In the Suru Valley, large amounts of volcaniclastic and some limestone blocks are included in the Dras Volcanic Group. In the eastern part of the ISZ in Ladakh, the Nindam Formation is a thick volcaniclastic sedimentary succession (Bassoullet *et al.* 1978, 1981; Colchen *et al.* 1986). The Dras volcanic rocks are interpreted as representing Jurassic–Lower Cretaceous island-arc volcanism above a N-dipping subduction zone within Tethys.

The Dras Volcanic Group is associated with a volcano-sedimentary succession, the Nindam Formation (Bassoullet *et al.* 1978). To the south and west of Rusi-la, agglomerates and tuffs with subordinate intrusive basalt are interbedded with shales and some bedded limestone that have yielded Cenomanian Foraminifera (I. Reuber, personal communication 1987). East of Trezpone, these limestones are compatible with a slope facies, containing conglomerates and graded beds of probable turbidite origin.

To the east, near Lamayuru, thick-bedded, graded volcaniclastic sandstones are interpreted as the products of high-density turbidity current deposition, and are interbedded with finergrained low density turbidity current graded sands, silts and shales. Diagenetic remobilization of silica has resulted in the silicification of shales. Sediments of the Nindam Formation are interpreted as being derived from the Dras volcanic arc (Fuchs 1977; Thakur 1981).

(*d*) *Indus Group molasse*

A continental clastic sequence approximately 2000 m in thickness, comprising alluvial fan, braided stream and fluvio-lacustrine sediments, constitutes the Indus Group (Brookfield & Andrews-Speed 1984*a*, *b*; Van Haver 1984). Clasts in the conglomerates were derived mainly from the uplifted and eroded Ladakh batholith to the north, but also from the suture zone itself (cherts, limestones, serpentinised peridotites) and from the Zanskar shelf carbonates to the south. Palaeocurrents show dominantly east to west basin axis-parallel sediment transport paths (Pickering *et al.* 1987). Near Kargil the Indus molasse unconformably rests on the Ladakh granitoids along the northern margin of the ISZ (figure 7*c*, plate 1).

The collision of India with the Karakoram and Lhasa Blocks and the closing of Tethys at 50 Ma marks the initiation of Indus Group molasse sedimentation (Searle *et al.* 1987). The Chogdo Formation at the base of the molasse rests stratigraphically above late Palaeocene shallow marine Sumda Formation limestones (figure 3). A *Nummulites*-bearing limestone interval (mid-upper Ilerdian–Cusinien (Van Haver 1984) marks the final marine incursion, and the ages of subsequent molasse deposits are poorly constrained, although they probably extend up into the Miocene (Tewari & Sharma 1972). The structure of the Indus molasse is dominated by late Tertiary N-directed backthrusting.

Figure 5 is a balanced cross section across the Indus Suture Zone along the Zanskar River section. Restoration of the late stage (T3) thrusts along this section (figure 6) indicates a minimum post-middle Miocene shortening of 36 km and an original minimum width of the Indus molasse basin of 60 km.

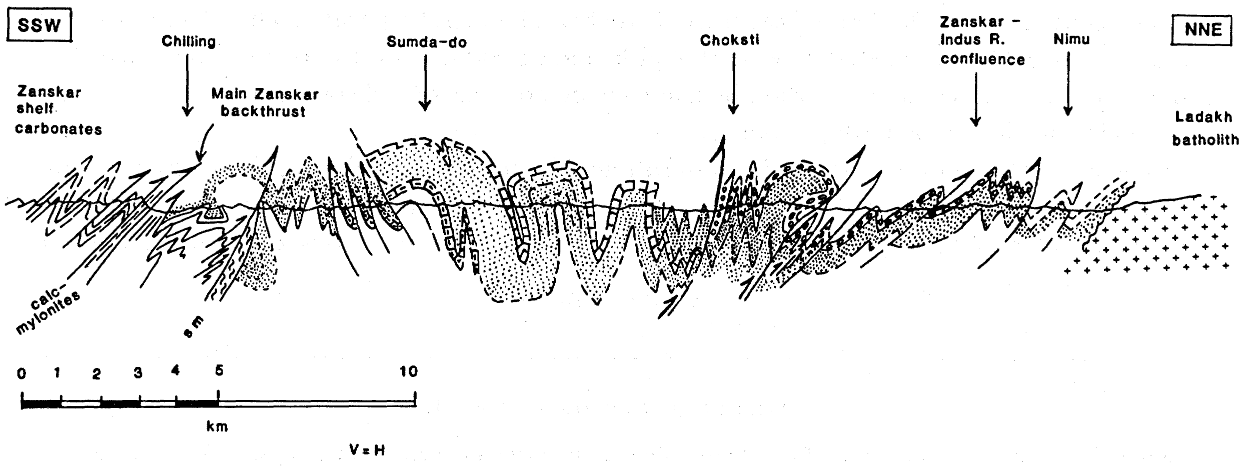

FIGURE 5. Structural section along the Zanskar River between Chilling and Nimu about 40 km west of Leh.

(*e*) *Subduction-related metamorphism*

Imbricated slices of blueschists occur in the Shergol ophiolitic mélange between the Dras volcanic thrust sheets to the north and the Lamayuru complex thrust sheets to the south. They are associated with a complex series of metabasic, volcaniclastic and sedimentary (dominantly

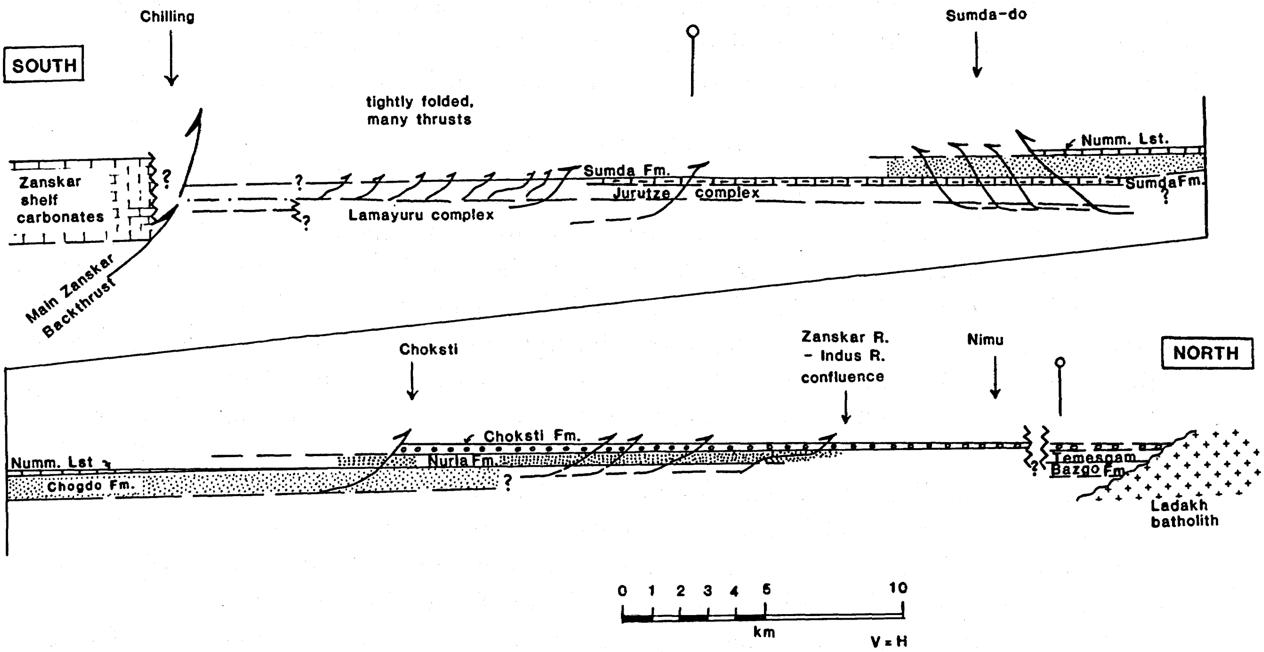

FIGURE 6. Restored section of the Indus Group along the Zanskar River shown in figure 5. The section has been restored sequentially along the Sumda Formation, the Nummulitic limestone and the Choksti Formation. The Jurutze complex is from data of Brookfield & Andrews-Speed (1984*a*).

red chert with some oolitic limestones) rocks and have a characteristic mineral assemblage: glaucophane–crossite–lawsonite–albite–phengite–chlorite–garnet–stilpnomelane–sphene, which indicate temperatures of formation of 400–450 °C at 10–12 kbar† (Honegger *et al.* 1985). These authors have found rare omphacite (jadeite contents 60–40 %) and quote middle Cretaceous ages from K–Ar analysis of whole rocks and mineral separates. These rocks crop out along a narrow belt immediately west of Sapi-la and extend for at least 10 km along strike. The blueschists are immediately overlain by a narrow belt of sheared red continental conglomerates belonging to the Indus Group molasse.

The restoration of thrust sheets in western Ladakh and Zanskar places these rocks at depths of around 30 km between the Lamayuru complex and the Nindam–Dras thrust sheets. We therefore infer that the site of major oceanic subduction was along this zone during the late

† 1 kbar = 10^8 Pa.

DESCRIPTION OF PLATE 1

FIGURE 7. (*a*) Panorama across the Indus Suture Zone from above the Lamayuru gompa. Z, Zanskar shelf; L, Lamayuru complex; O, ophiolitic mélange; N, Nimdam Formation; M, Indus molasse; Lb, Ladakh batholith. All units dip towards S and are backthrust towards N. (*b*) The Shergol ophiolitic mélange with glaucophane-bearing blueschists (B), overlain by Indus molasse (M), north of Sapi-la. This belt of mélange separates the Lamayuru complex (L) from the Dras Volcanic Group (DV). (*c*) Indus molasse (IM) unconformably overlying the Ladakh batholith (LG) and overthrusted by the Dras Volcanic Group (DV) along a N-directed backthrust. North of Kargil. (*d*) Upright anticline in the Indus molasse along the Zanskar River section. The lower molasse unit, the Chogdo Formation (Ch) is overlain by the marine *Nummulitic* limestone (Numm) and the continental molasse of the Nurla Formation (N). (*e*) Conglomerates of the Hemis Formation in the Indus molasse. Light-coloured pebbles are Ladakh granites, andesites and dacites, dark pebbles are serpentinites and red cherts.

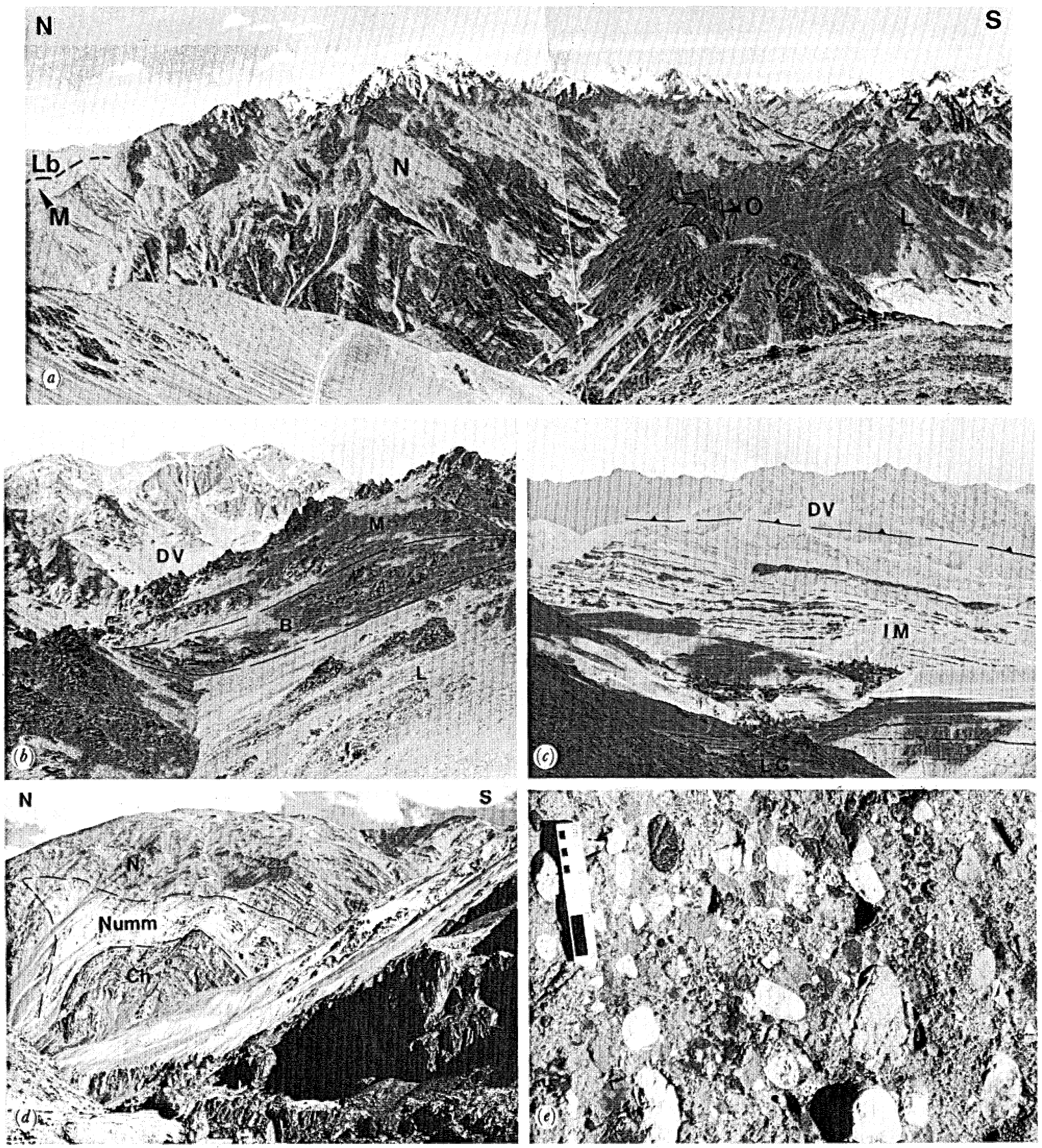

FIGURE 7. For description see opposite.

(*Facing page* 126)

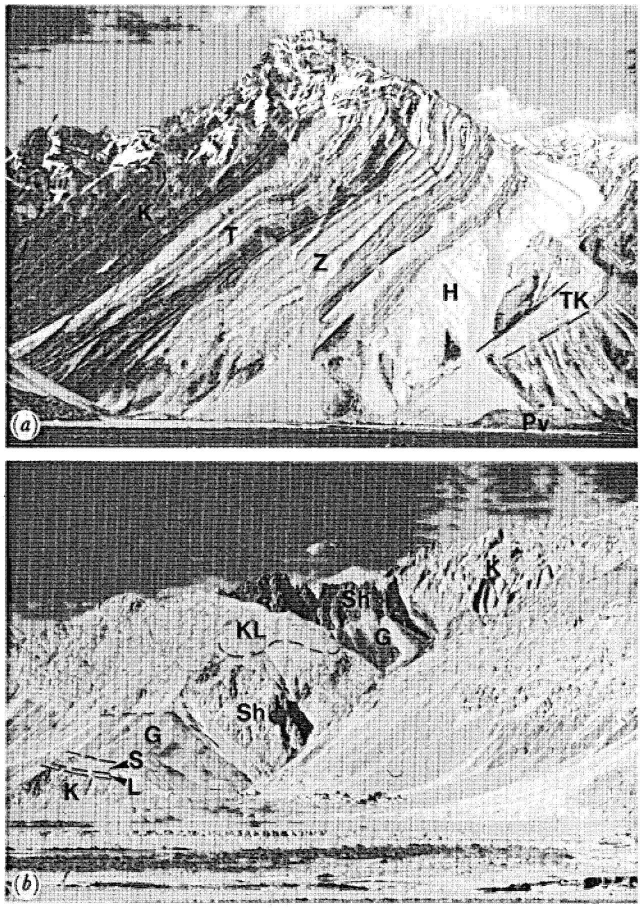

FIGURE 8. Zanskar Supergroup stratigraphy exposed at (*a*) Rangdum and (*b*) Zangla. Pv, Panjal Volcanic Group; TK, Tamba Kurkur; H, Hanse; Z, Zozar; T, Tsatsa; K, Kioto; L, Laptal; S, Spiti; G, Guimal; Sh, Shillakong; KL, Kanji-la Formations.

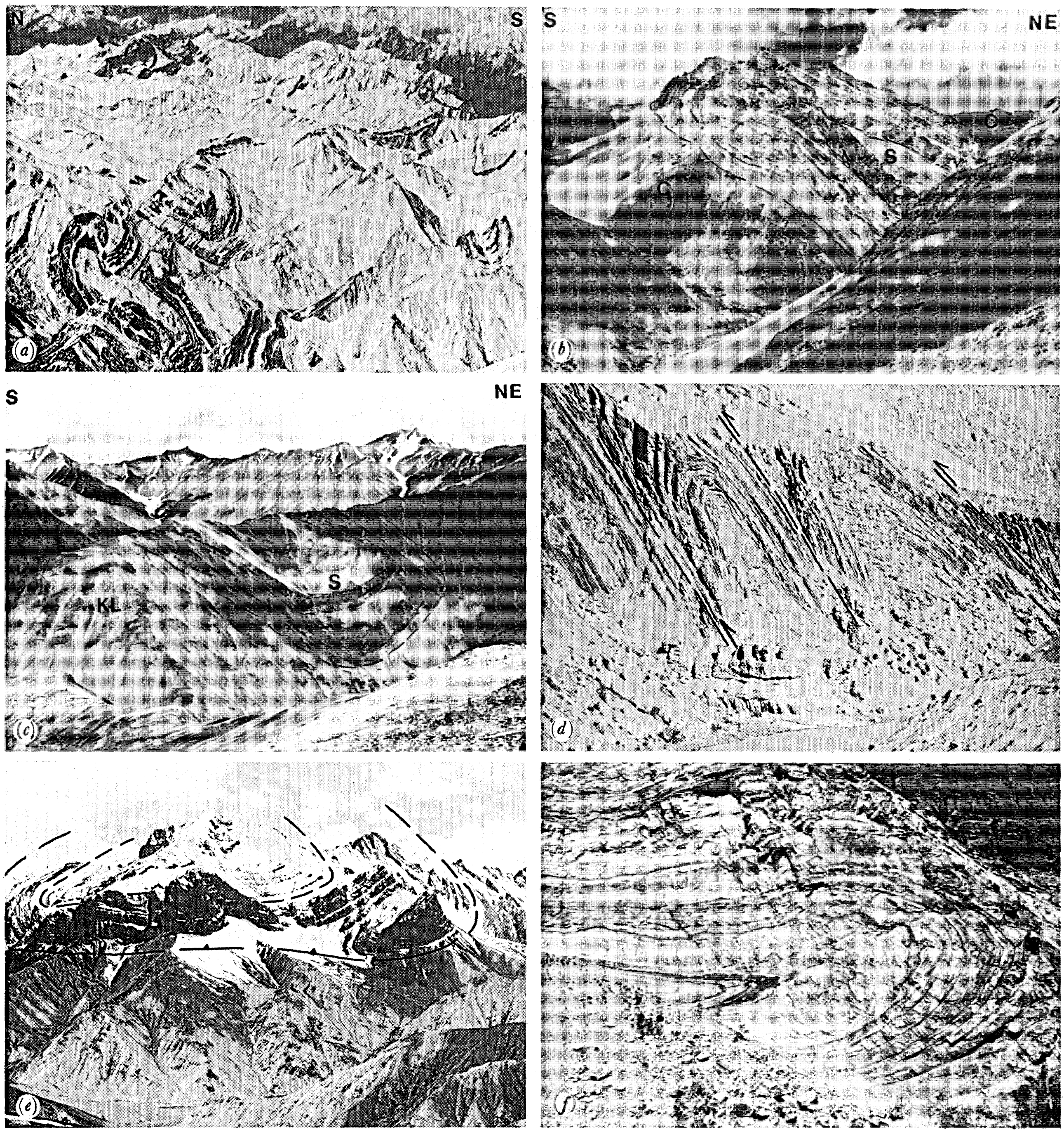

FIGURE 15. (*a*) Aerial view looking east across the northern part of the Zanskar shelf showing the northern Zanskar 'pop-up' structure with N-facing folds in the N and S facing folds in the south. (*b*) SW-facing isoclinal fold in Spanboth Formation (S) marine limestones and Chulung-la Formation (C) continental slates, N of Dibling. (*c*) SW-facing syncline in Kanji-la Formation (KL) and Spanboth Formation (S) limestones, near Kanji-la, western Zanskar. (*d*) Tight to isoclinal SW-verging folding and imbricate thrusting in Lilang group limestones, Zanskar River, N of Zangla. (*e*) Giant sheath fold in the Mesozoic shelf carbonates of the northern Zanskar unit. View S from Rubering-la, eastern Zanskar. (*f*) Isoclinal fold in Zozar Formation limestones with flat-lying axial plane, in the western Zanskar zone of lateral spreading, unnamed southern tributary of Wakka Chu, near Shergol.

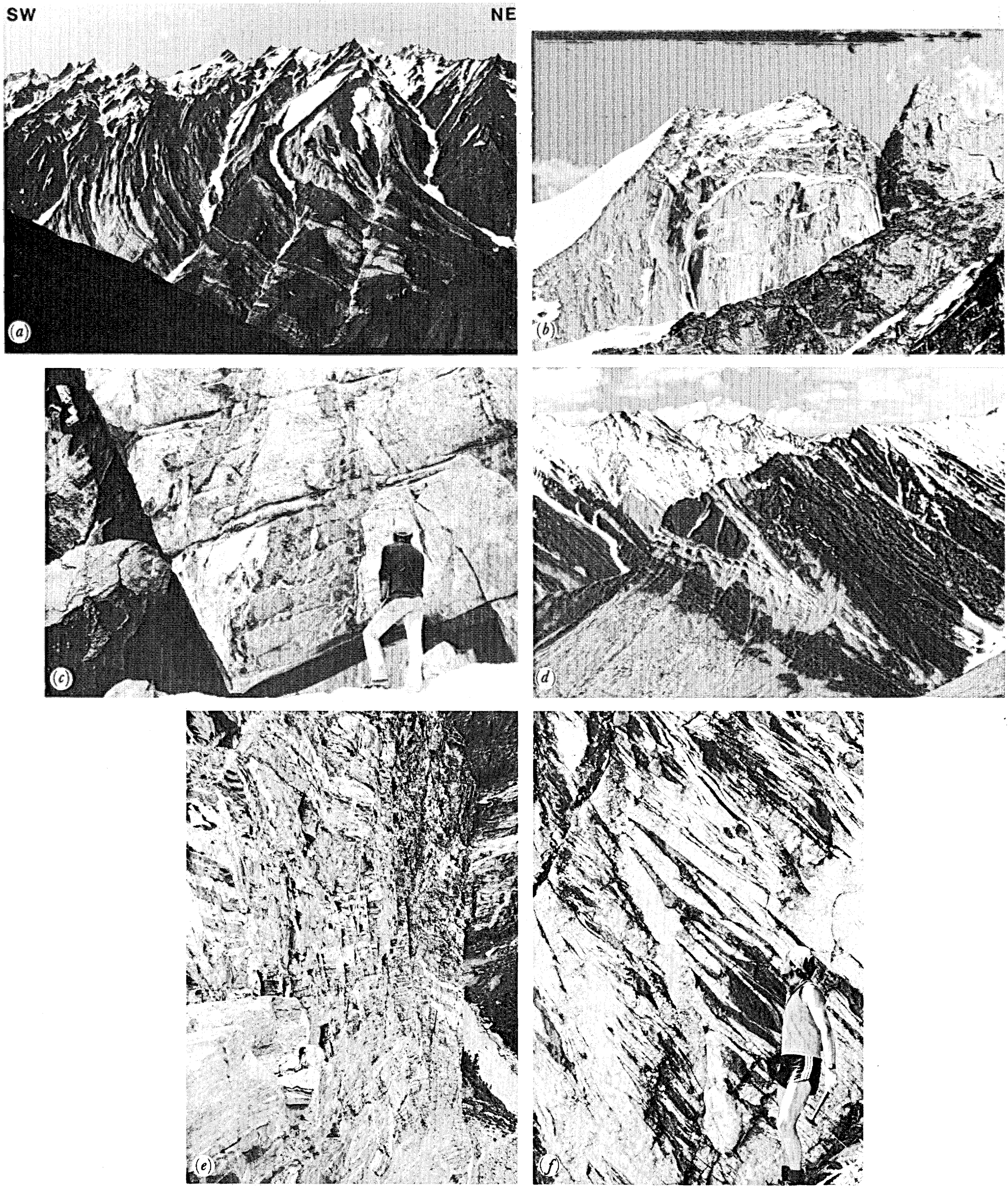

FIGURE 16. For description see opposite.

Cretaceous and Palaeocene (figure 4) with the oceanic crustal slab subducting to the north beneath the Dras island arc. Blueschists are also present on the hangingwall of the MMT in Kohistan (Shams 1980; Shams *et al.* 1980) and are dated at 80 ± 5 Ma (^{39}Ar–^{40}Ar) by Maluski & Matte (1984). Bard (1983) has related the high-pressure metamorphism in Kohistan to the southward obduction of the Kohistan island arc sequence during the late Cretaceous.

In eastern Ladakh, Virdi *et al.* (1977) and Jan (1985) have described glaucophane–epidote–garnet–rutile–stilpnomelane–actinolite–quartz–albite assemblages with uncommon lawsonite in metabasic rocks in the ISZ that are associated with the Nidar ophiolite complex (Thakur 1981).

(*f*) *Structural evolution*

The structure of the Indus Suture Zone is complex and involves pre-collision oceanic thrusting associated with obduction of the Dras–Kohistan arc, and obduction of the Spontang ophiolite and associated sub-ophiolitic sheets. Additionally, continuous deformation from closure of the suture (50 Ma) to the present has been incurred. The early phases of thrusting are difficult to recognize because of subsequent extreme deformation during and after closure.

The presence of glaucophane, lawsonite and (?)omphacite in the Sapi-la blueschists indicate that they were formed at minimum pressures of around 10 kbar, corresponding to depths of around 30 km in an oceanic subduction environment (figure 4). Rapid thrust exhumation of these rocks is implied for them to retain their blueschist mineralogy without being thermally reset by decreasing P–T. Their incorporation into the ophiolitic mélange along with unmetamorphosed sedimentary and volcanic blocks must have been a shallow-level process. Late Cretaceous thrusting of the Lamayuru complex and Dras arc is also implied by the Santonian–Maastrichtian age on the ISZ ophiolitic mélanges and the ages of the blueschists in Ladakh and Kohistan (figure 3).

A major phase of SW-directed thrusting occurred along the north Indian continental margin during the Santonian to Palaeocene (80–60 Ma). Thrusts in the Lamayuru complex are not continuous upwards into the late Palaeocene-Eocene rocks. Two marine transgressions during the Upper Palaeocene (Sumda Formation) and lower Eocene (*Nummulitic* limestones) were responsible for final marine Tethyan sedimentation before ocean closure at *ca.* 50 Ma (figure 7*d*, plate 1). Thick continental molasse overlies the Lower Eocene limestones and the whole sequence has been deformed by dominantly upright folding and N-directed backthrusting after deposition of the molasse (late Miocene–Pliocene, figure 3). Along the northern part of the ISZ the Indus molasse rests unconformably on the eroded Ladakh batholith (figures 5 and 6).

Description of plate 4

Figure 16. (*a*) Amphibolites, marbles and meta-pelites in a SW-verging recumbent nappe, the Donara nappe, looking N from Bobang Gali, eastern Kashmir, W of Panikar. (*b*) Upper intrusive contact of a Himalayan granite in zone 4, east of Kun. (*c*) Lower thrust contact of a sheet intrusive leucogranite in zone 3, Suru Valley near Shafat. Note ductile foliation bending into the thrust plane at base of the granite. (*d*) The Zanskar Shear Zone north of the Pensi-la showing condensed isograd sequence associated with normal faulting. (*e*) The anatectic zone 1 granite-leucogranite zone along the Chenab Valley near Dharwas. White bands are garnet–muscovite–tourmaline leucogranites, dark bands are sillimanite or kyanite-bearing gneisses. (*f*) Isoclinal folding and ductile shearing in a leucogranite mixing zone within sillimanite grade gneisses, Suru Valley.

5. Zanskar Shelf Zone

(a) *Stratigraphy of the Tibetan-Tethys Zone*

Early reconnaissance studies of the Zanskar Range were made by Lydekker (1883), Gupta & Kumar (1975), Nanda & Singh (1977), Fuchs (1977, 1979, 1982) and Sharma & Kumar (1978). The present stratigraphic framework is largely based on these works and also those of Gaetani *et al.* (1980, 1983, 1985), Kelemen & Sonenfeld (1983), Baud *et al.* (1984) and Garzanti *et al.* (1986).

A Lower Palaeozoic orogenic cycle has been identified by Garzanti *et al.* (1986) and is marked by passive margin, shallow water and tidal flat, terrigenous and dolomitic sequences (Phe and Karsha Formations) passing up into Upper Cambrian deep-water shales and turbidites (Kurgiak Formation) which are overlain by Ordovician continental molasse conglomerates and sandstones (Thaple Formation). Subsequent Palaeozoic sedimentation is represented by the Devonian aeolian sandstones of the Muth Formation, Early Carboniferous limestones and evaporites (Lipak Formation), and marine deltaic clastics (Po Formation). These units collectively comprise the Lahoul Supergroup.

The Zanskar Supergroup (figure 8, plate 2, and figure 9) represents sedimentation on the north Indian Plate margin from the inception of Neo-Tethyan rifting in the Permian to final collision of the Indian Plate with the Karakoram–Lhasa Blocks of the southern Eurasian Plate. Rift-related continental tholeiitic volcanics and volcaniclastics (Panjal Volcanic Group) rest unconformably on the Precambrian to Carboniferous sediments of the Lahoul Supergroup, although this contact has been locally modified by normal faulting associated with the Zanskar Shear Zone.

Following an early clastic phase (Kuling Formation), rapid deepening of the newly formed continental margin resulted in a shallowing-upward sedimentary sequence, from outer-shelf argillaceous limestones with minor carbonates (Tamba Kurkur and Hanse Formations) to shallow water carbonate environments (Zozar, Tsatsa and Kioto Formations) (figure 8*a*, plate 2).

Carbonate platform evolution ended in the middle Jurassic (? Bathonian) and, following a 10 Ma hiatus, a condensed sequence of ferruginous oolites, sandstones and shales accumulated (Laptal Formation; Jadoul *et al.* 1985), overlain by thin Oxfordian–Lower Cretaceous shales of the Spiti Formation, representing the local response to a regional Tethyan deepening event (figure 8*b*, plate 2). Coarser clastic input (Guimal Formation) up until the Albian marked the end of passive margin sedimentation patterns, and subsequent sedimentation is interpreted as a response to the late Cretaceous obduction of the Spontang ophiolite.

During the Cenomanian–Turonian, deep-water, nodular limestones (Chikkim Formation) were deposited in an interior continental margin environment, whereas along the platform margin, collapse of the continental margin caused an erosion surface to cut down to the Kioto Formation, above which deeper-water pelagic limestones (Shillakong Formation) were deposited. Intraformational unconformities and conglomerate horizons indicate increasingly unstable conditions along the continental margin. A rapid increase in sedimentation rates during the Campanian is recorded in the Kanji-la Formation (Gaetani *et al.* 1983), and is modelled as a response to foredeep development ahead of the Spontang ophiolite. The Kanji-la Formation is a diachronous, prograding sequence of hemipelagic marls and turbidites, which

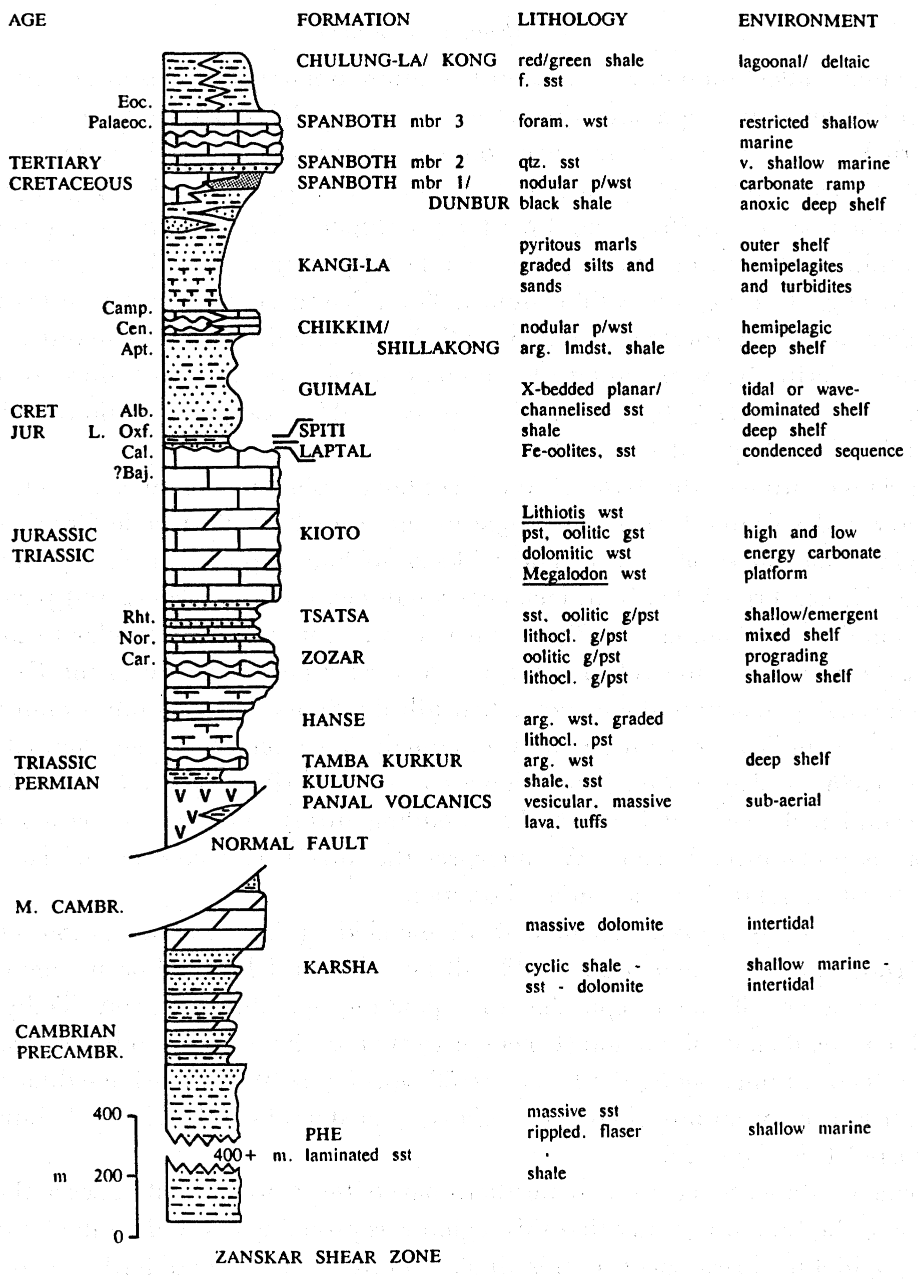

FIGURE 9. Compilation of the stratigraphy of the Zanskar Range based largely on Fuchs (1979, 1982), Gaetani *et al.* (1983, 1985), Baud *et al.* (1984), and Garzanti *et al.* (1986).

is Campanian in the margin interior (SW) and Maastrichtian along the northern Zanskar shelf. A return to shallow water conditions is marked by the localized northwards progradation of a Maastrichtian carbonate ramp (Spanboth Formation, member 1) into an anoxic shale basin (Dunbur Formation). The Lower Palaeocene is missing in Zanskar (Gaetani *et al.* 1983) whereas above the unconformity the Spanboth (members 2 and 3)–Lingshet Formation is well dated by Foraminifera as Upper Palaeocene–Lower Eocene (Gaetani *et al.* 1983).

(*b*) *Spontang allochthon*

The Spontang allochthon in western Zanskar, approximately 30 km south of the ISZ (figure 10) comprises an upper ophiolite thrust sheet tectonically overlying thrust sheets of Dras volcanic rocks, mélanges and Lamayuru complex that were emplaced southwestwards on to the Zanskar shelf (Fuchs 1982; Kelemen & Sonnenfeld 1983; Searle 1983, 1986; Reuber 1986; Colchen *et al.* 1986). The Spontang ophiolite (*sensu stricto*) comprises a harzburgite–dunite–lherzolite mantle sequence overlain by cumulate gabbros and wehrlites and a poorly developed sheeted dyke–sill complex. The volcanic component has a MORB chemistry and the complex is interpreted as a slab of Tethyan oceanic crust and mantle. Pyroxenite, gabbro and dolerite dykes intruding the ophiolite provide poorly constrained K–Ar ages on amphiboles of $156–127 \pm 10$ Ma (Reuber *et al.* 1987). Serpentinization and calcium–metasomatism is widespread.

The mélange around the base of the Spontang ophiolite contains a wide variety of sedimentary and volcanic blocks that range in age from Permian to late Cretaceous (Fuchs 1979, 1982; Colchen *et al.* 1987). These blocks include Upper Permian platform-related carbonates, Upper Triassic Hallstatt facies carbonates with alkaline lavas, and Jurassic pelagic limestones and radiolarian cherts. The Triassic exotic limestones are similar to the Mulbeck exotics in the ISZ and some volcanic blocks are similar petrologically to the Dras Volcanic Group. The shaley matrix of the mélange beneath the Spontang ophiolite contains abundant *Globotruncana* sp., indicating a Santonian–Campanian (late Cretaceous) age (figure 3) (Colchen & Reuber 1986). Colchen *et al.* (1987) have recently described Lower Eocene Foraminifera from a second mélange unit beneath the Spontang thrust, and on this basis interpret the obduction as post-Lower Eocene. We interpret this thrust as a late, out-of-sequence, post-collision thrust, unrelated to the initial obduction.

Fuchs (1977, 1979, 1982), Kelemen & Sonnenfeld (1983), Reuber (1986), Colchen & Reuber (1986) and Kelemen *et al.* (1988) all favour a post-Lower Eocene age of ophiolite obduction. However, if one accepts that the Spontang ophiolite represents Tethyan oceanic crust and mantle, then its obduction (Coleman 1971) must have occurred before ocean closure, which is well constrained along the ISZ as *ca.* 50 Ma (figure 3). No marine sediments younger than Lower Eocene occur anywhere on the Zanskar shelf or along the ISZ and obduction must have occurred before 50 Ma.

No Tertiary sediments occur on the northern part of the Zanskar shelf between the Spontang ophiolite and the ISZ, suggesting that this region was probably covered by the Lamayuru and Spontang ophiolite thrust sheet at this time. Indeed, south of Bodkharbu, poorly exposed Lamayuru complex slates and limestones, with associated alkali basaltic sills, structurally overlie black slates and calcareous slates assigned to the Dunbur Formation (facies transitional to the Kanji-la Formation), implying probable Maastrichtian emplacement of the Spontang ophiolites.

Gaetani *et al.* (1983) have shown that extremely rapid sedimentation rates are recorded in the Kanji-la Formation, and Brookfield & Andrews-Speed (1984*a*) demonstrate the existence of a foredeep along the Zanskar continental margin during the late Cretaceous. We interpret this foredeep as the inboard response to loading of Tethyan thrust sheets on to the continental margin during a late Cretaceous obduction event. Obduction-related thrusting propagated from NE to SW and may have spanned 20 Ma (from 80 to 60 Ma; figure 3), comparable to the span of emplacing the Oman ophiolite and Bay of Islands, west Newfoundland ophiolite (Searle & Stevens 1984; Searle 1985, 1986, 1988).

(*c*) *Pre-collision thrusting*

In the Zanskar Range, pre-collision (T1) thrusts are now only preserved within later, post-collision (T2, T3) thrust-bounded duplexes, and can only be demonstrated in the area around the Spontang ophiolite (figures 10 and 11). In this area at least three major phases of thrusting can be determined by simple cross-cutting relations. The recognition of out-of-sequence and breakback thrusts is crucial to the interpretation of tectonic events.

The Lamayuru complex rocks exposed in T1 thrust sheets around the base of the Spontang ophiolite are distal oceanic sediments (red radiolarian cherts and shales) and mélanges. The shaley sequences are hard to distinguish from the overlying Kanji-la and Dunbur Formations. However, the great thickness observed on the north side of the Spontang ophiolite when compared with the known stratigraphic thickness of the Dunbur Formation further to the west (*ca.* 150 m in Wakka Chu and Kangi Chu) suggests the presence of Lamayuru complex rocks below the ophiolite. A Jurassic ammonite from between the Spontang ophiolite and Photoksar thrust near the Spong River (Brookfield & Westermann 1982) further suggests these rocks belong to the Lamayuru complex. These shales extend westwards as narrow thrust-bounded slices towards Kanji (figures 12 and 13) where they are of more proximal oceanic facies (Goma Formation; figure 4). Thrust slices of Lamayuru rocks exposed at Singe-la (figure 10) tectonically overlie the complete Mesozoic shelf sequence along thrust contacts (T1) that pre-date the unconformably overlying Lingshet limestones (figure 11*a*). Restoration of the folding in the Palaeocene–Lower Eocene Lingshet Formation shows that folds and thrusts in the Mesozoic sequence are not continuous upwards into the Lingshet limestones (figure 11*b*). A major phase of shortening therefore occurred during the late Cretaceous, before deposition of the late Palaeocene–early Eocene shallow marine carbonates.

The same Lamayuru complex rocks exposed at Singe-la tectonically underlie the Spontang ophiolite and slices of Jurassic–Lower Cretaceous Dras volcanics and mélanges around the margin of the Spontang Klippe. The pre-collision stacking order of thrust sheets around Spontang is directly comparable to that of the well-exposed and better-studied ophiolites such as the Oman and West Newfoundland examples, both of which were obducted on to passive continental margins. This tectonic stacking order during the T1 obduction phase is diagrammatically shown in the model presented in figure 14.

(*d*) *Post-collision thrusting*

Following continental collision between India and the Karakoram–Lhasa Blocks and closing of the Indus Suture Zone at 50 Ma, thrusting of the complete Zanskar shelf and its overlying Tethyan thrust sheets caused widespread crustal shortening and thickening south of the ISZ. Initially, major thrusts propagated southwestwards across the Zanskar shelf, in a piggy-back sequence of thrusting. The youngest rocks affected by this deformation are the late Palaeocene–early Eocene Spanboth and Chulung-la Formations in the west (figure 15*a*, *b*, plate 3), and the Lingshet and Kong Formations in the east.

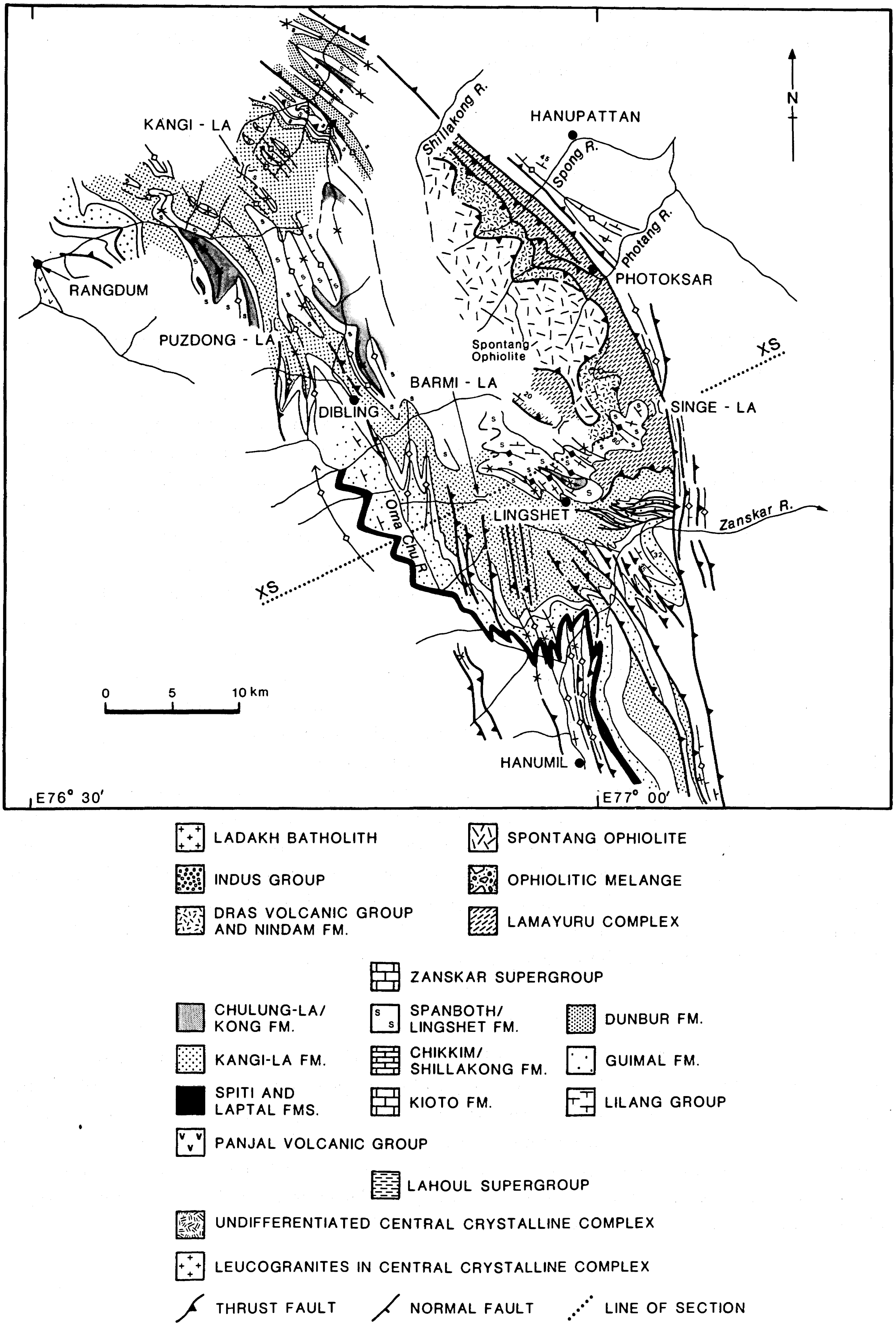

FIGURE 10. Geological map of the area around the Spontang ophiolite.

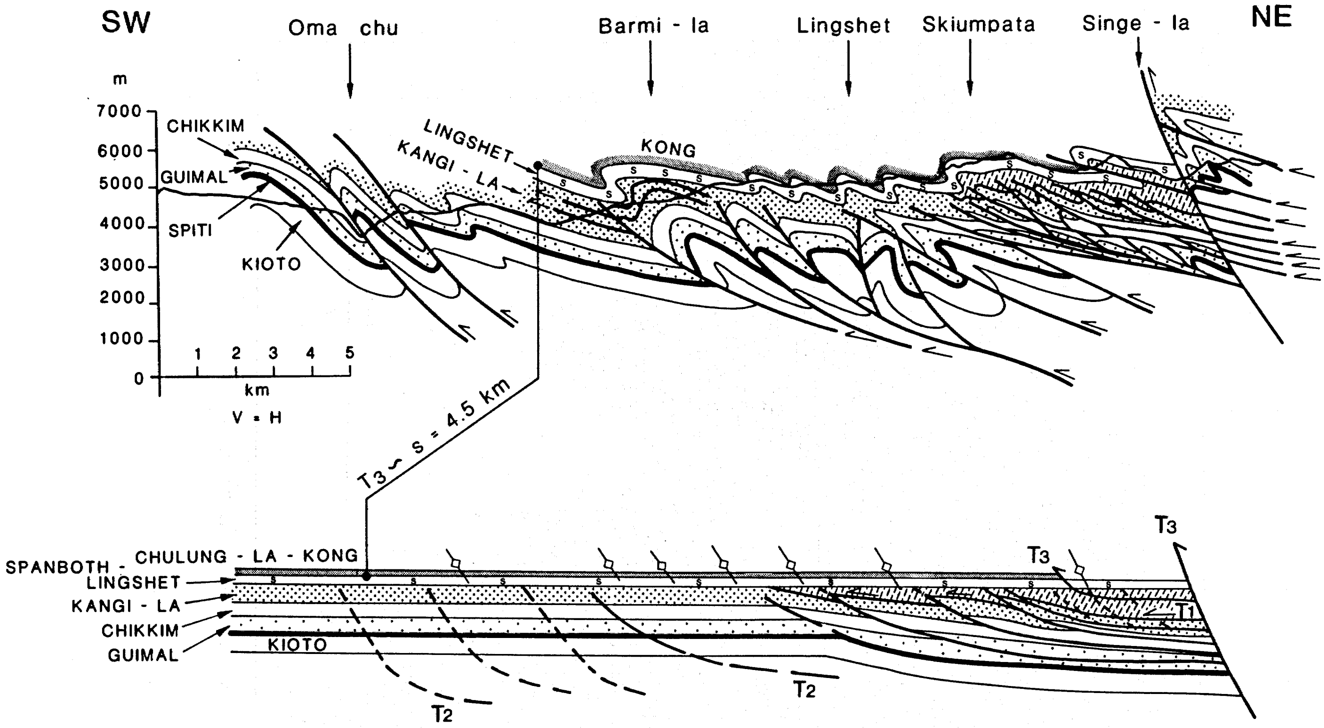

Figure 11. (*a*) Structural cross section and (*b*) partly restored section across the area shown in figure 10. The Photoksar thrust is the large-scale breakback thrust along the NE margin. T1, T2, T3 refer to thrust sequences described in text. Section (*b*) shows restoration of the post – lower Eocene folding and thrusting to show the obduction-related T1 and early collision-related T2 thrusts in the shelf sequence.

The structure of the Zanskar shelf sediments can be broadly divided into five zones (partly after Baud *et al.* 1984), each characterized by a differing structural style.

1. The Spontang Zone in western Zanskar is the only area where the pre-collision ophiolite obduction-related structures can be distinguished. These early thrusts (see previous section) are preserved within later SW-directed breakback thrusts such as the Photoksar thrust (figures 10 and 11), which truncates the earlier folds and thrusts along its footwall.

2. The Phugtal Zone along the SW margin is dominated by late NE-dipping normal faults associated with the Zanskar Shear Zone which downthrows Palaeozoic sediments on to sillimanite–kyanite grade gneisses of the High Himalaya (see following section). Earlier SW-facing folds (figure 15*c*, plate) have in places been refolded by upright and NE-facing folds which are associated with gravitational collapse in response to the Miocene Himalayan uplift to the SW.

3. The Zangla Zone is the zone of maximum compression in eastern Zanskar. Tight, isoclinal, non-concentric, flexural slip and flexural shear folds and steep SW-directed thrusts are dominant (figure 15*d*, plate 3). Out-of-sequence thrusts, placing younger rocks onto older, are inferred from a high degree of layer-parallel shortening and thickening.

4. The Northern Zanskar Zone along the north and northeastern margin is a 25–30 km wide 'pop-up' zone with steep SW-directed thrusts in the SW and steep NE-directed backthrusts along the NE. The SW-directed thrusts are related to the Photoksar breakback thrust (figure 11) and are late in the sequence. Backthrusting affects the northern part of the Zanskar shelf

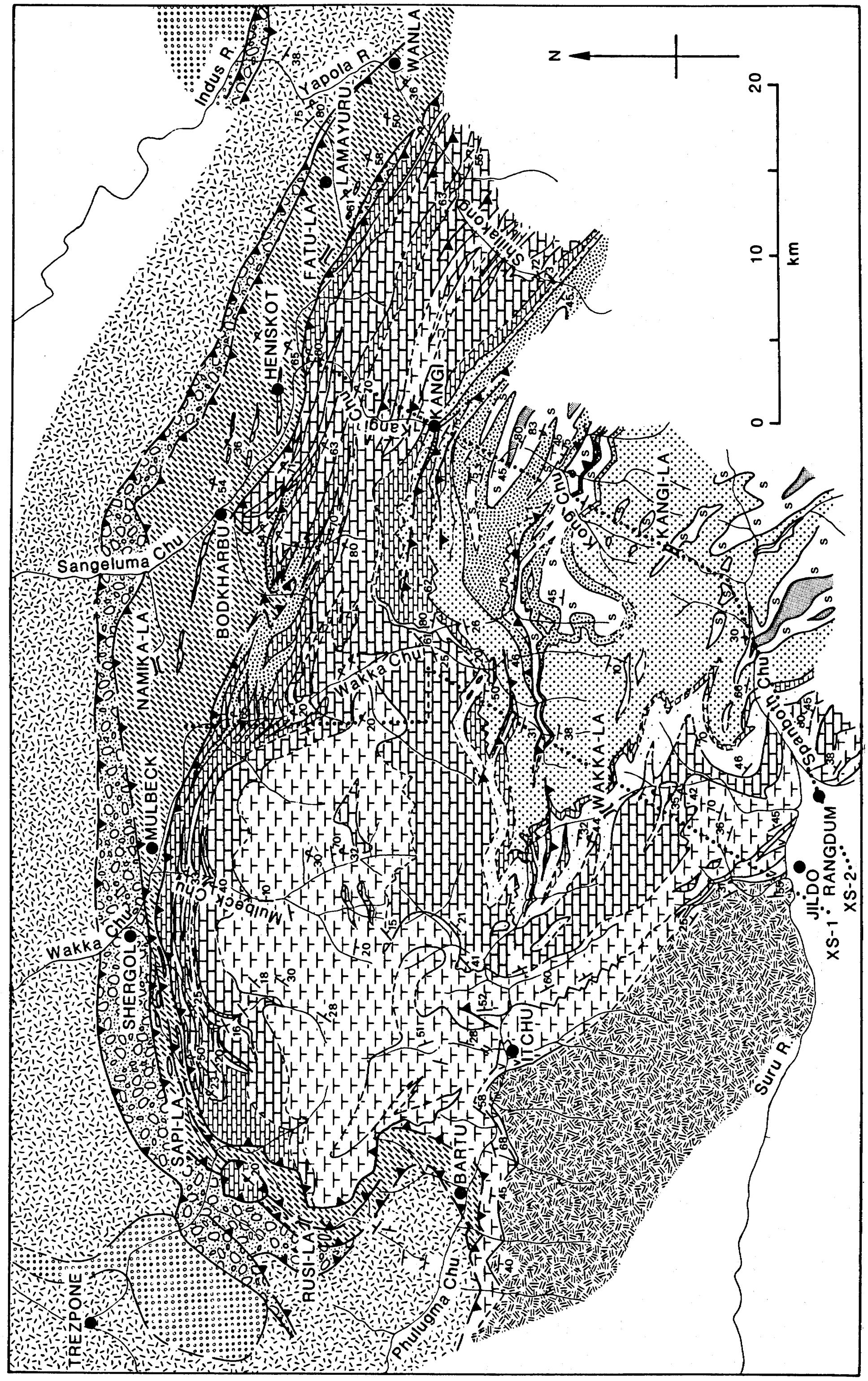

FIGURE 12. Geological map of western Zanskar. Key is same as for figure 10.

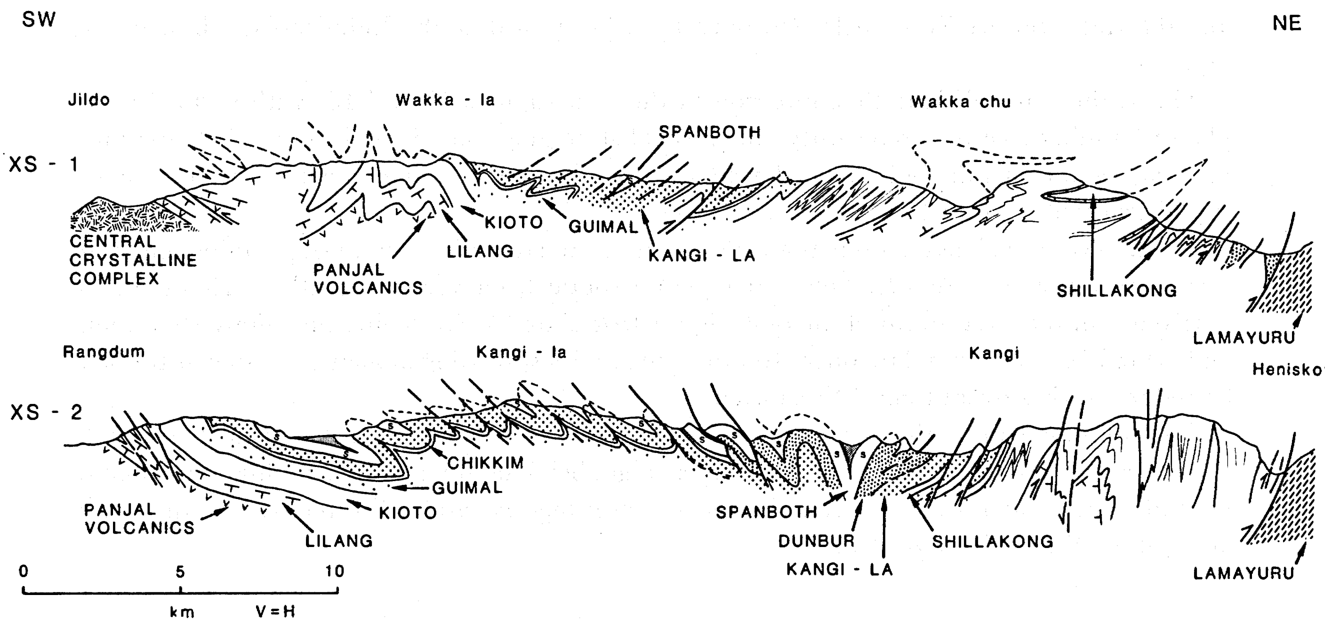

FIGURE 13. Cross section across western Zanskar, locations marked on figure 12.

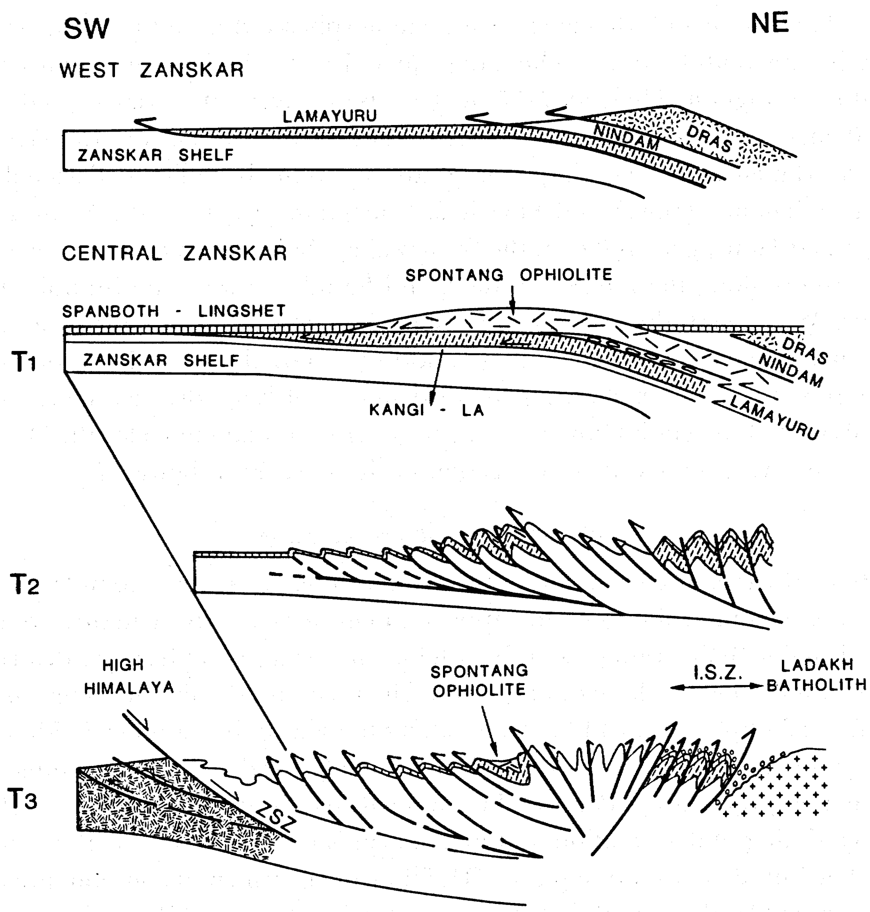

FIGURE 14. Schematic sections to explain the structural evolution of the Zanskar shelf structure. See text for discussion.

and the Indus Suture Zone rocks and must therefore post-date the Indus molasse in age (see figure 3).

This is the zone of highest compression in the west (figures 12 and 13) with vertical axial planes (fanning), vertical schistosity and vertical stretching lineations. In the NE (Rubering-la area), giant sheath folds have developed by progressive simple shear of original non-cylindrical folds (figure 15*e*, plate 3).

5. The Western Zanskar Zone is a zone of lateral (westward) extruding/spreading fold and thrust structures (figure 12). Fold axial planes rotate from vertical, south of Heniskot, to horizontal in the west, south of Shergol (figure 15*f*, plate 3). Stretching lineations are radial. Gilbert & Merle (1987) relate these structures to gravity spreading at a laterally unconstrained boundary during overall NE–SW shortening.

Post-collision deformation shows a multi-stage thrust evolution with cross-cutting breakback thrusts being particularly important, the later stages being dominated by culmination-collapse normal faulting along the SW margin and by late stage N- and NE-directed backthrusting along the NE margin (figure 14).

6. High Himalayan Zone

The High Himalayan Range, south of the Zanskar Valley (figures 2 and 17) is a zone of Precambrian, Palaeozoic and Mesozoic rocks metamorphosed during the climax of Himalayan deformation in the mid-Tertiary. The range includes the highest mountains in Ladakh–Zanskar, with the highest, Nun, at 7135 m. Because of over 50% glacier and snow coverage, and difficult access, it is the least-known zone of the Himalaya. Conventional mapping and three-dimensional mapping of isograds is extremely difficult. Selected areas have been studied by Thakur (1981) and Powell & Conaghan (1973) in the Kulu–Lahoul area, Searle (1983) and Honegger (1983) in the Suru Valley, Searle (1983), Searle & Fryer (1986) and Herren (1987) along the Zanskar Valley, and Kundig (1989) and Staubli (1989) in the Kishtwar area. We have studied the area in eastern Kashmir–western Zanskar along the Suru, Doda, Kargyiak, Chenab and Kulu Valleys and in the Tos glacier region around White Sail (figure 2). Figure 17 is a map showing the distribution of isograds, metamorphic zones and granites in this part of the High Himalaya. Figure 18 is a thermal model for the High Himalaya south of Zanskar based on a scale cross section of the area from figure 17.

(*a*) *Structure and metamorphism*

The relation between deformation and metamorphism is very complex in the High Himalaya Zone. Metamorphic isograds appear to cut across early structures but have been folded around major SW-verging recumbent folds indicating two phases of deformation, one before and the other after peak metamorphism. The rocks are dominantly meta-pelites with a high proportion of amphibolites and marbles along the Kashmir–Zanskar divide west of Nun-Kun. These represent the westernmost exposure of the Central crystalline complex until their reappearance along the Nanga Parbat–Haramosh Range in northern Pakistan (figure 2).

The relative timing of deformation and metamorphism is shown in the Tertiary time chart in figure 19. The initial deformation phase, D1, following continental collision, involved crustal thickening through SW-directed thrust stacking. Associated regional Barrovian metamorphism (M1) constitutes a prograde medium P–T event reaching kyanite grade metamorphic

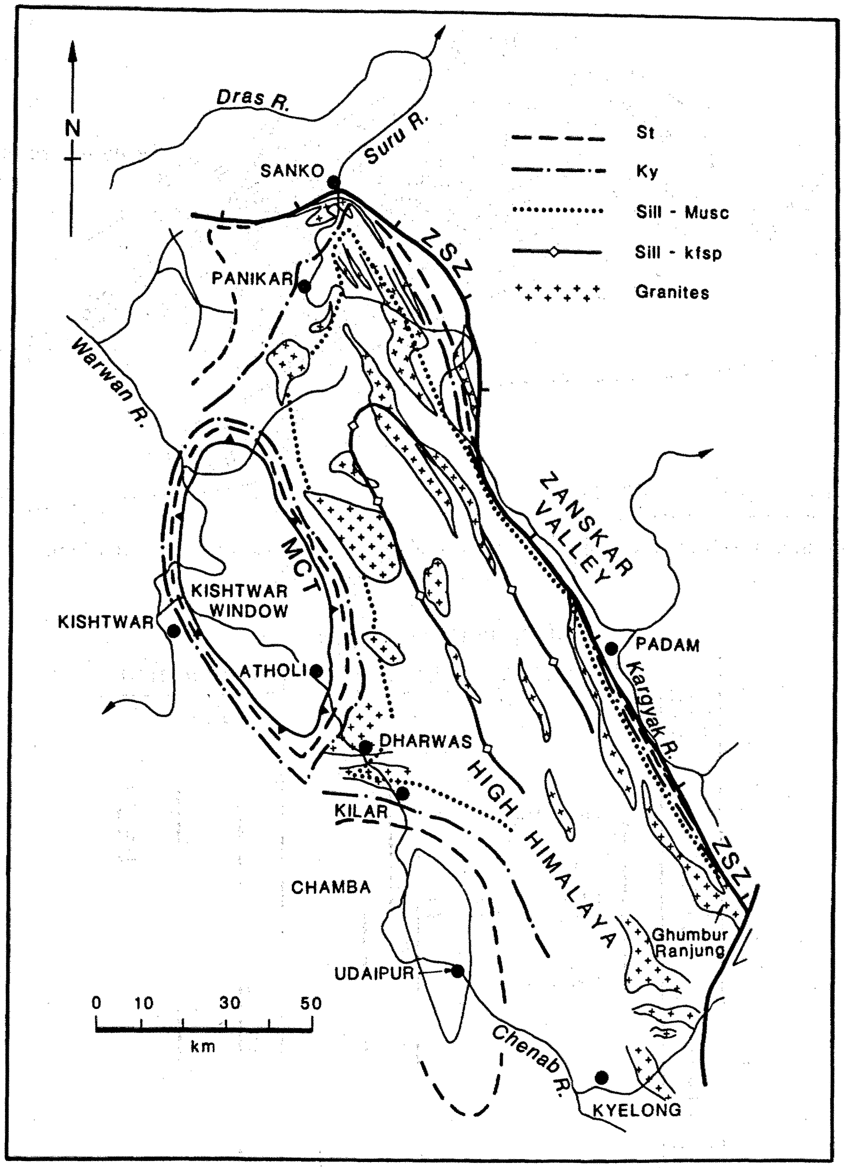

FIGURE 17. Metamorphic map of the Zanskar–Chamba–Kulu area of the High Himalaya showing approximate distribution of isograds from geologic mapping of Honegger (1983), Searle & Fryer (1986), Herren (1987), Staubli (1989), Kundig (1989), and this work. MCT, Main Central Thrust; ZSZ, Zanskar Shear Zone. St = staurolite, Ky = kyanite, Sill = Sillimanite, Musc = muscovite, kfsp = K-feldspar.

conditions. M1 assemblages are overprinted by a second stage of kyanite growth, fibrolite sillimanite and biotite (Staubli 1989; Kundig 1989). This M2 stage indicates an increase in temperature and/or a decrease in pressure. It is roughly contemporaneous with major SW-directed recumbent folds and thrusts along the Main Central Thrust (MCT) Zone.

The M2 event is contemporaneous with the onset of partial melting in the sillimanite zone and the generation of melt pods and leucogranitic sheets. Migmatites with *in situ* leucogranitic segregations are widespread in the deepest structural levels along the central part of the High Himalayan Range, around Dharwas in the Chenab Valley (figure 17) and the Manali–Tos glacier region in the SE. Continual NE–SW compression during the Oligocene–Miocene

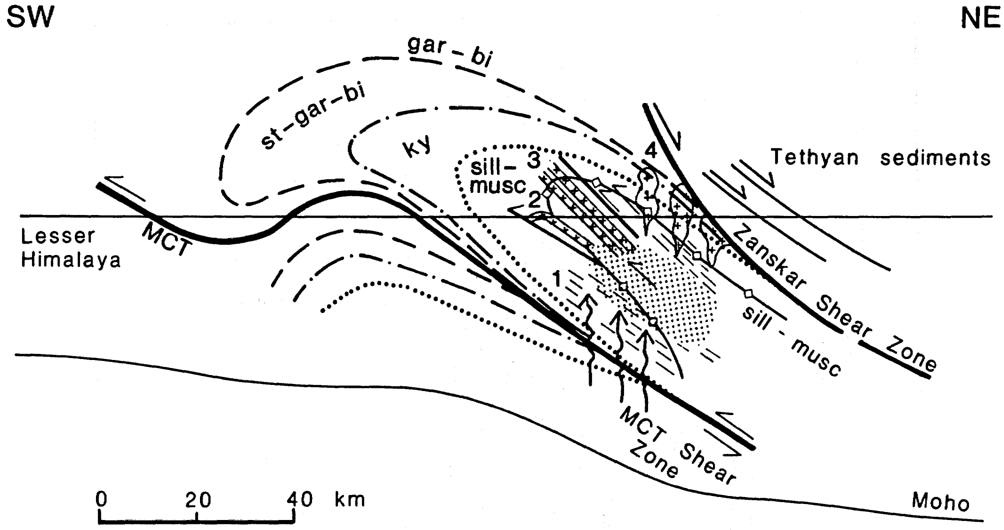

FIGURE 18. Thermal model for the High Himalaya in Zanskar proposed and discussed here, based on a scale cross section of figure 17.

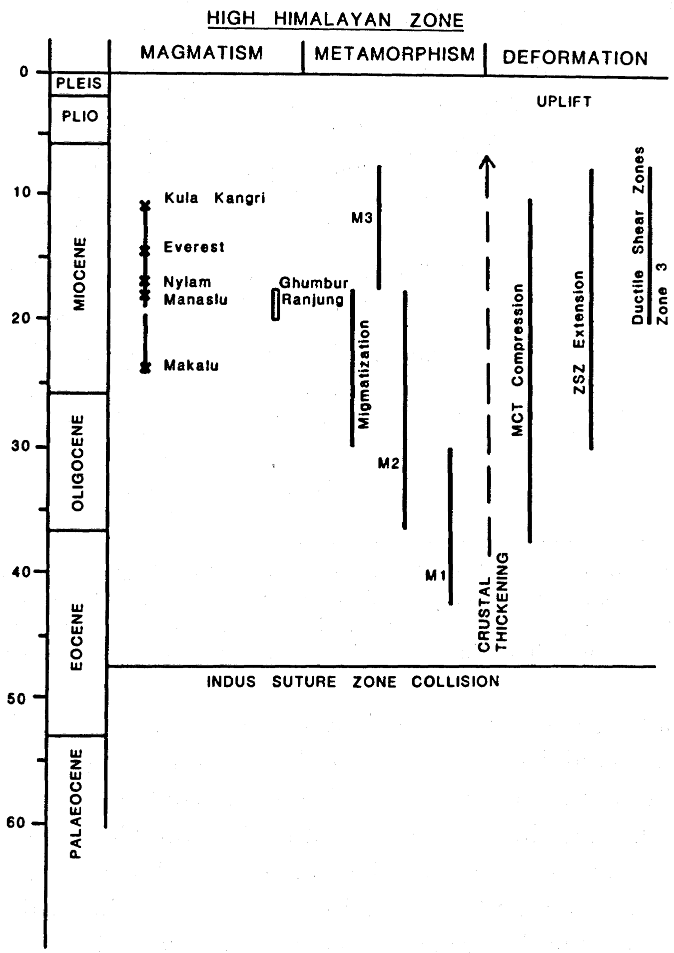

FIGURE 19. Tertiary time chart for deformation, metamorphism and magmatic events of the High Himalaya. Crosses represent U–Pb zircon, monazite ages. Ghumbur Ranjung is Rb–Sr age. See text for sources of data.

resulted in a cycle of NE-directed underplating, SW-directed overthrusting, metamorphism and partial melting at the highest P–T conditions and subsequent exhumation on later SW-directed thrusts (D2). NE-dipping extensional faulting at upper crustal levels is also inherent to the thrust system. M3 is a retrograde metamorphism due to decreasing P–T conditions during uplift or thrust culmination. Rapid uplift on SW-directed MCT-type thrusts preserved the inverted metamorphic isograds seen around the Kishtwar window (Staubli 1989); they are also described from the MCT Zone in Nepal (Le Fort 1975; Pêcher 1975; Caby *et al.* 1983) and Darjeeling (Sinha-Roy 1982).

The higher structural levels of the High Himalayan Zone can be seen to the west of Nun-Kun (figure 17). In eastern Kashmir–western Zanskar, three large SSW-verging recumbent folds or nappes are separated by ductile shear zones or brittle thrust faults. The isograds appear to be folded around these structures creating an inverted metamorphic profile in the lower limbs. The uppermost nappe (Sanko nappe) consists of garnet-biotite leucogranite in the core of a recumbent fold. The southernmost of these folds is the Donara nappe (figure 16*a*, plate 4) where interbanded pelites, marbles and garnet amphibolites are folded into a S-verging, SW-plunging nappe.

(*b*) *Himalayan crustally derived granites*

Granites and leucogranites of the High Himalayan Zone south of the Zanskar Valley and along the Suru Valley are lithologically diverse and consist of K-feldspar + plagioclase + quartz + biotite ± muscovite ± garnet ± tourmaline. Most of these granites are considered to be Himalayan–Miocene in age. Older granites (possibly Cambrian) also occur in the High Himalaya and frequently form the cores of granite gneiss domes in the central part of the range (Le Fort *et al.* 1986; Kundig 1989). These older porphyritic granites are mantled by migmatites, probably of Himalayan age, within the sillimanite zone (figure 18).

Many compositional varieties of leucogranites occur along the Suru Valley and south of the Zanskar Valley, including garnet–biotite granite, K-feldspar megacrystic two-mica ± garnet leucogranite and tourmaline leucogranite. Tourmaline is rarer in these leucogranites than in other Himalayan leucogranites, such as Manaslu and Bhagirathi. South of the Zanskar and Kargyak Valleys, garnet–tourmaline–muscovite leucogranites occur, and near Dharwas in the Chenab Valley (figure 17) kyanite is also present in the 'lit-par-lit' injection granites (Searle & Fryer 1986).

Himalayan granites and leucogranites are spatially restricted to the sillimanite and kyanite zones but narrow dykes or sheets may extend up into the staurolite or garnet zones. We propose here that the granites and leucogranites within the High Himalayan Zone in the western Himalaya occur in four main tectonic settings. The four morphostructural granite types are schematically illustrated in the thermal model shown in figure 18. Zone 1 corresponds to the proposed location of partial melting within the sillimanite–muscovite and sillimanite–K–feldspar metamorphic terrane. Anatexis occurs at depths of *ca.* 15–30 km, at temperatures in the region of 600–750 °C and pressures of 4–5 kbar (400–500 MPa) (Searle & Fryer 1986; Pinet & Jaupart 1987). The composition and mineralogy of the *in situ* granites are dependent upon the composition of the source protolith and the ambient P–T–X (H_2O) conditions. The amount of water available in the zone of partial melting is controlled by the localized metamorphic environment and by the abundance of externally derived fluid. The migration of volatile-enriched fluid derived from the cool, hydrous Lesser Himalayan slab, underlying the hotter High Himalayan slab, may be effective in lowering the 'wet' granite solidus. The migmatite terrane occurs along the highest peaks of the High Himalayan Range and deeper levels of migmatites and layered granitic melts are well exposed along the Chenab Valley near Dharwas (figure 16*e*, plate 4).

Zone 2 melts are incipient migmatitic mantles around the porphyritic granite gneiss domes, exposed for example around the Umasi-la, and N of the Kishtwar Window (Kundig 1989). The structural relationships indicate that these older (? Cambrian) porphyritic granites form a considerable component of the melting source for the Miocene leucogranites.

Zone 3 granites are the sheet intrusives, dominantly leucogranitic, that are well exposed along the Suru Valley. They have been thrust up to higher structural levels on fluid-rich ductile shear zones as a result of melt-enhanced deformation (Hollister & Crawford 1986) that juxtaposed rocks of different metamorphic grades and crustal levels. Along the Suru Valley these granites occur as NE-dipping sheet-like intrusions parallel to the regional schistosity in the surrounding sillimanite–garnet–biotite gneisses. Upper contacts are generally intrusive (figure 16*b*, plate 4) whereas basal contacts are brittle thrust faults (figure 16*c*, plate 4) or ductile shear zones often with migmatites and complex mixing zones in the hangingwalls (figure 16*f*, plate 4). Strain generally increases downwards within a leucogranite sheet and kinematic indicators (C–S fabrics, asymmetric pressure shadows around garnet or feldspars) in the gneisses indicate SW-directed thrusting, except along the top of the High Himalayan slab where brittle normal faults show displacement down to the NE. Some leucogranites show a high degree of internal ductile strain (figure 16*f*, plate 4), and are recumbently folded, indicating that intrusion and cooling were synchronous with the mid-Tertiary SW-verging folding and thrust culmination of the High Himalaya.

Zone 4 leucogranites are the higher-level migrated plutons exemplified in this area by the Ghumbur Ranjung pluton (figure 17) in SE Zanskar (Searle & Fryer 1986; Pognante *et al.* 1987). These plutons have actively migrated into higher structural levels of the High Himalayan crystalline slab and thus cross-cut the metamorphic isograds. Conditions of maximum thermal conductivity contrast exist along the footwall of the Zanskar Shear Zone (figure 18), which separates low thermally conductive Tethyan sediments from the high thermally conductive gneisses of the High Himalayan Zone (Jaupart & Provost 1985; Pinet & Jaupart 1987).

The Ghumbur Ranjung pluton is a garnet–muscovite–biotite–tourmaline leucogranite with a Rb–Sr (mica) isochron age of 20.7–18.4 $\pm$ 0.6 Ma and an initial $^{87}Sr/^{86}Sr$ ratio of 0.747–0.775 (Ferrara *et al.* 1986), which compares closely with many other Miocene Himalayan leucogranites (Le Fort *et al.* 1987). A preliminary Rb–Sr (whole rock–muscovite) age of 17.6 Ma was obtained on a tourmaline–muscovite coarse-grained leucogranite–adamellite from near Bardan gompa, 10 km SE of Padam (Searle & Fryer 1986). These Miocene dates (figure 19) are compatible with the well-dated leucogranite plutons of Makalu, 24 Ma (Schärer 1984); Manaslu, 25–18 Ma (Deniel 1985; Le Fort *et al.* 1987); Nyalam, 17 Ma; Everest, 14 Ma; and Kula Kangri, 11 Ma (Schärer *et al.* 1986).

It is important to dismiss the view that all granitic melts generated from intracrustal metasedimentary sources are of low-temperature, minimum-melt composition. All of the granitic–leucogranitic lithologies observed in the Suru Valley section, for example, may be derived from the melting of crustal protoliths. The amount of melting, the chemistry of the melts and the residue will depend not only on the composition of the protolith, but also upon the water budget of the source that is undergoing partial melting.

The lowest temperature, near minimum-melt leucogranites are produced under prograde metamorphism resulting from the breakdown of muscovite. However, higher-temperature melting involving biotite breakdown reactions in high-grade metasediments will also produce granites and leucogranites, but of variable, 'non-minimum' melt composition. The fluid content of the magma defines its mobility and emplacement level in the crust. Furthermore, the heat availability will have important consequences for melting with, for example, higher temperature melt fractions being produced from a source that has previously undergone a partial melting episode. These later melt fractions will be of a distinctly 'non-minimum' melt composition. As the thermal budget is of prime importance in the petrogenesis of High Himalayan melts, and localized thermal heterogeneity is strongly suspected (Pinet & Jaupart 1987; Hodges *et al.*, this symposium), a variety of granite compositions are likely to be produced in this tectonic environment.

(*c*) *Main Central Thrust Zone*

The existence of a major crustal-scale shear zone placing the high-grade rocks of the High Himalaya over the low-grade rocks and sediments of the Lesser Himalaya has long been known (Heim & Gansser 1939; Le Fort 1975). However, the exact location of the Main Central Thrust (MCT) with respect to the inverted metamorphic isograds is constantly disputed. Valdiya (1980) places it at the top of the Central Crystalline Complex (Vaikrita thrust) in Kumaon, Sinha-Roy (1982) places it at the base of the inverted metamorphic sequence in Darjeeling, and others place it along the kyanite isograd in Central Nepal (Le Fort 1975; Pêcher 1977). All these authors define the MCT on lithological or metamorphic conditions rather than strain. We prefer to define the MCT as a ductile shear zone *ca.* 5 km wide along which there are several zones of high strain with mylonites at higher levels. Brunel (1986) shows that the minimum translation on the MCT in the Everest–Makalu region is around 100 km.

The field relations in the High Himalaya of Zanskar, Kishtwar, Chamba and Kulu (figures 2 and 17) clearly indicate that the metamorphic isograds have been deformed by a later phase of SW-verging folding and thrusting. In eastern Kashmir–western Zanskar, the location of the MCT is contentious. It follows approximately the base of the Donara nappe around the Boktol Pass west of Panikar (figure 17) but further west has been rotated by subsequent thrust movements in the footwall to become vertical, and in places possibly even backthrusted, so that the Kashmir Palaeozoic–Mesozoic sediments have been re-thrust during D3 northwards over the metamorphic rocks of the Donara nappe.

Around the Kishtwar window, metamorphic isograds have been telescoped during SW-directed thrusting (Staubli 1989) and folded by subsequent lower thrust culminations of the Lesser Himalayan sheets. Searle & Fryer (1986) describe a decrease in metamorphic grade in eastern Zanskar–Lahoul southeastwards to the Chenab valley where Powell & Conaghan (1973) found Jurassic microfossils in low-grade marble at Tandi. The isograds have clearly been folded around the Chamba syncline and the Kishtwar anticline. Stretching lineations, in general, are aligned NE–SW, parallel to the displacement direction.

There are three main models to explain the inverted metamorphic isograds of the Himalaya. The first is the rapid thrusting of the hot High Himalayan slab on to a colder Lesser Himalayan slab (Le Fort 1975). The result of this would be downward decreasing P–T conditions away from a major thrust plane in the footwall and upward decreasing retrogressive metamorphism in the hangingwall. Extremely rapid thrust rates and uplift–exhumation rates are implied in order to preserve the inverted metamorphism without thermal re-equilibration.

The second model involves two-stage metamorphism: an earlier emplacement of a 'hot'

High Himalayan hangingwall on to a 'cold' Lesser Himalayan footwall at intermediate pressures (kyanite grade) followed by higher T–lower P (sillimanite grade) metamorphism related to granitic magmatism. We feel it is unlikely that any thermal imprint from partial melting would be so spatially extensive (up to 50 km away from the nearest granite source region). We also discount the effect of any shear heating involved outside the immediate vicinity of high-strain shear zones, mainly because of the extensive fluid and volatile fluxing within the High Himalaya.

The third model involves deformation of an earlier Barrovian metamorphic sequence with upward decreasing P–T conditions by later crustal-scale folds and ductile shear zones. The result of this would be both downward (inverted limb of fold) and upward (upper limb) decreasing initial P–T conditions. Unlike the Nepal and Darjeeling sectors of the Himalaya, the Zanskar area does show the upper limb with upward decreasing isograds (figure 18), and we therefore favour this third model to explain the inverted metamorphism.

(*d*) *Zanskar Shear Zone*

The contact between the High Himalayan crystalline rocks and the sediments of the Zanskar shelf sequence is a N-dipping normal fault zone (Searle 1986; Herren 1987). The fault extends along the 100 km long Zanskar Valley (figure 2) and separates Barrovian facies metamorphic rocks, migmatites and leucogranites in the south from Palaeozoic–Mesozoic sediments and Panjal volcanics in the north. Metamorphic isograds are structurally telescoped along the contact where a transition from upper amphibolite facies (sillimanite–K-feldspar gneisses) to lower greenschist facies occurs within 200 m. The normal fault reaches a maximum offset in the central part of the area around Padam (figure 17). Herren (1987) calculated a minimum horizontal extension of 16 km and a minimum vertical displacement of 19 km in this region. Towards the west along the Suru Valley (figure 16*d*, plate 4), isograds widen as the throw on the fault decreases. The axis of maximum P–T conditions is parallel to the fault zone approximately 20 km south of the Zanskar Valley along the highest mountains of the Himalayan Range.

The Zanskar Shear Zone offsets all the rocks of the High Himalaya including the Miocene leucogranites. Garnet–muscovite–tourmaline leucogranites from the footwall of the Zanskar shear zone have K-Ar ages on micas (muscovite blocking temperature *ca.* 350 °C, biotite *ca.* 300 °C) of 30 ± 2 and 22 ± 1 Ma (D. C. Rex, personal communication). Kinematic indicators such as C-S fabrics and feldspar augen consistently indicate the shear sense as being northeast side down (Herren 1987). Stretching lineations are generally NE–SW or N–S and plunge north. No indications of strike-slip motion have been found along the Zanskar Shear Zone.

The trailing edges of many thrust culminations are bounded by extensional normal faults although none have been described on such a large scale as the Zanskar Shear Zone. Searle (1986) interpreted this fault as a dorsal culmination collapse feature associated with, and synchronous with, rapid thrusting and uplift in the High Himalaya and MCT Zone to the south. The NE–SW extension is probably confined only to the upper crustal levels and does not imply extension in the lower crust (figure 18). Structural analysis of the High Himalaya and fault-plane solutions of earthquakes (Seeber *et al.* 1981; Molnar 1984) indicate only compressional tectonics in the High and Lesser Himalaya. This also implies that the Zanskar Shear Zone is listric and flattens out to the north into a mid-crustal detachment. This may also explain why there is no typical Indian lower crust (granulites) exposed in the Himalaya (see §7).

The same normal fault can be traced for 900 km eastwards across the Annapurna Range in Nepal (Le Fort 1975; Pêcher 1977; Caby *et al.* 1983) and across southern Tibet (Burg & Chen 1984; Burg *et al.* 1984). The low-angle, N-dipping normal fault along the northern flanks of Everest and at Nyalam on the Kathmandu–Lhasa road cuts Oligocene metamorphic rocks and leucogranite sheets dated radiometrically at 30–15 Ma (Allègre *et al.* 1984) and must therefore have been active during Miocene–Pliocene times (Burchfield & Royden 1985).

The thermal conductivity contrast across the ZSZ between sediments of low thermal conductivity on the hangingwall and gneisses and granites of high conductivity along the footwall (Jaupart & Provost 1985) is also important in maintaining a maximum heat flux at the top of the High Himalayan slab. The sediments of the Zanskar shelf would have acted as a thermal barrier to the upward transport of heat and could explain the concentration of Himalayan leucogranites at the top of the slab.

7. Discussion

(a) *Thrust sequences*

It is clear that although the overall structural framework of the Himalayan collision is one of southward propagating thrusting from the ISZ in the north to the MCT Zone and MBT in the south, numerous complications arise. The ISZ has undergone compression since the mid-Eocene collision and is now dominated by steep N-directed backthrusts that post-date the Indus Molasse Group and must therefore be late Miocene to (?)Pliocene in age. Earlier SW-directed thrusts in the Lamayuru complex must have been passively rotated by underthrusting and continued compression so as to dip steeply to the south. Subsequent compression during the backthrusting phase has reactivated these faults as N-directed thrusts. The resulting internal folding and cleavage can therefore be extremely complex and difficult to restore fully. This rotation of earlier thrusts and folds also resulted in a tectonic inversion of the earlier stacking order and the widespread rethrusting of the Zanskar shelf rocks northwards over the ISZ rocks.

The structural evolution of the Zanskar shelf involves a continuum of crustal shortening and thickening by thrust stacking since collision at *ca.* 50 Ma. Within this continuum, cross-cutting thrust relations indicate that out-of-sequence and breakback thrusts are extremely important, particularly in the northern part of the Zanskar Range. Thrusts associated with the obduction of the Spontang ophiolite are the earliest in the sequence and are cut off along their trailing edges by late breakback thrusts that cut through the whole tectonic stack (Searle 1986). These late breakback thrusts are thought to be contemporaneous with the steep N-directed backthrusting creating a 25–30 km wide 'pop-up' zone along the northern margin of the Zanskar shelf.

Very tight to isoclinal folding within the Mesozic shelf carbonates suggests that major bedding-parallel detachments occur along the less competent horizons. For example, the Kioto Formation limestones in the Zangla zone are deformed mainly by intra-formational isoclinal folding with large-scale detachments along the underlying relatively incompetent beds of the Lilang Group below, and the Laptal and Spiti Formations above. This style of thrusting results in homogenous crustal thickening with thrusts placing younger rocks on to older.

The deformation in the High Himalayan zone southwest of the Zanskar Valley is characterized by ductile folding and numerous SW-directed ductile shear zones. The higher crustal levels around the Suru Valley and eastern Kashmir show SW-verging recumbent folds that are bounded by major shear zones involving Barrovian facies metamorphic rocks. The deeper structural levels in the core of the range show that crustal thickening occurred through flow folding and migmatization with remobilization of leucosome material. Syn- or post-metamorphic thrusting along the MCT Zone at the base of the slab and concomitant NE-directed culmination collapse normal faulting along the ZSZ have both resulted in telescoped metamorphic isograds. Rapid thrust rates in the High Himalaya during the late Oligocene–Miocene coupled with tectonic denudation on the NE dipping normal fault system along the ZSZ resulted in rapid uplift and preservation of the inverted metamorphism along the base of the slab and the high-grade metamorphic and anatectic core along the top of the slab. Post-metamorphic folding of isograds during SW-directed MCT-thrusting can be demonstrated in western Zanskar (figures 17 and 18).

(*b*) *Crustal shortening*

The amount of crustal shortening across the ISZ and Zanskar shelf can only be estimated by the restoration of balanced cross sections. The section across the ISZ along the Zanskar River (figures 5 and 6) indicates 36 km of post-Indus molasse shortening, on restoration of the late-stage T3 thrusts and folds. Lack of sufficiently detailed stratigraphical and structural data at present makes it impossible to restore the pre-molasse sediments.

A balanced and restored cross-section across the Zanskar shelf and ISZ east of the Zanskar River shows that the present 98 km width from the Zanskar Valley normal fault to the Ladakh batholith restores to 250 km, implying shortening of 152 km (Searle 1986; Searle *et al.* 1987) of which 112 km is accommodated by shortening of the Zanskar shelf units. Shortening estimates from the western (Rangdum–Kanji-la section, *ca.* 56 km) and the eastern (Marang-la–Phugtal section, *ca.* 36 km) part of the Zanskar Range are considerably less (Searle & Cooper, in preparation). These balanced cross-section reconstructions have several constraining factors, notably: (1) trailing edges of thrust sheets are rarely seen; (2) depth-to-basal detachments are not known; (3) folding is dominantly flexural slip or flexural flow, rarely parallel or concentric; (4) differing amounts of layer-parallel shortening are commonly observed between incompetent shaley beds that deform by internal thickening and competent limestones that deform by folding; and (5) strain rates increase towards the north, where ductile flow folding is observed.

No attempt has yet been made to determine the amount of shortening across the High Himalaya. Very complex ductile strain in these metamorphic rocks and anatectic granites makes it impossible to restore any cross section. The P–T estimates for these rocks in the High Himalaya also suggest a complex Tertiary thermal history with evidence of multi-stage thrusting and crustal thickening, accompanied by NE-dipping normal faults at upper crustal levels. Shortening estimates from the Lesser Himalaya in Kashmir, Chamba and Kulu are also unknown although preliminary mapping in eastern Kashmir suggests only minor shortening (34 km) in the section from the Vale of Kashmir to the Central crystalline complex (Searle & Cooper, unpublished data).

Despite major pre-collision palaeogeographic differences, the continuity of Himalayan thrust systems between India and Pakistan allows some comparisons to be made. Coward & Butler (1985) and Coward *et al.* (1987) constructed a balanced cross section from the MMT southwards to the Punjab foreland in an attempt to quantify the amount of crustal shortening in the Pakistan Himalaya. The rocks of the Indian Plate in this section restore to at least 720 km with an implied shortening of 470 km and they, and Butler (1986), argue for large-scale underthrusting of Indian lower crust beneath Kohistan and the Karakoram northwards to the Pamirs.

Our shortening estimates for the Zanskar shelf sequence must be matched by a similar amount of shortening in the lower and middle crust. In common with most present-day passive continental margins with relatively thick shelf sediments, the continental crust beneath the pre-collision Zanskar shelf was probably considerably thinner than the average 35 km thickness of the Indian foreland crust. This decreases the necessity for large-scale underthrusting of Indian crust beneath Tibet.

(c) *Crustal subduction*

Balanced cross sections of the Ladakh–Zanskar Himalaya indicate that some crustal subduction must have occurred. The major question is how much, and how far northwards has it gone? The low density and great thickness of continental crust suggests that it is too buoyant to be subducted unless it was greatly attenuated (McKenzie 1969). However, Molnar & Gray (1979) suggested that if the upper and lower crust could be detached, the lithospheric mantle could be cold and dense enough to subduct the lower 10 km of continental crust. In the Himalaya, the MCT Zone could be considered as a mid-crustal plane along which such detachment may have occurred. Major whole crustal detachments as suggested by Molnar (1984) or crust–mantle detachments (Mattauer 1986) for the Himalaya can account for the shortening estimates (*ca.* 250 km) in the Zanskar–Ladakh Himalaya (figure 20) but could not account for the 470 km shortening across the Pakistan section estimated by Coward & Butler (1985) assuming standard 35 km thick crust. Either the 470 km shortening is an overestimate, or large volumes of Indian lower crust must have been subducted northwards, to achieve a crustal balance, or else the crust was greatly thinned prior to thrusting. Butler (1986) invoked a model of eclogite metamorphism in the subducting plate to facilitate this large-scale continental subduction, based on the radical difference in density across the metamorphic phase boundary between granulite–amphibolite and eclogite (Richardson & England 1979). In this model the subducting continental plate would be metamorphosed to dense eclogite and the geophysical Moho might only represent this phase boundary, making an area balance of the continental crust impossible.

Our model for the structural evolution of the Western Himalaya in India is based on the crustal-scale cross section shown in figure 20. This figure has been constructed with the deep crustal constraints of Lyon-Caen & Molnar (1983) and Molnar (1984), but also includes the Zanskar shelf and ISZ structure from Ladakh. The crustal thickness is known to be

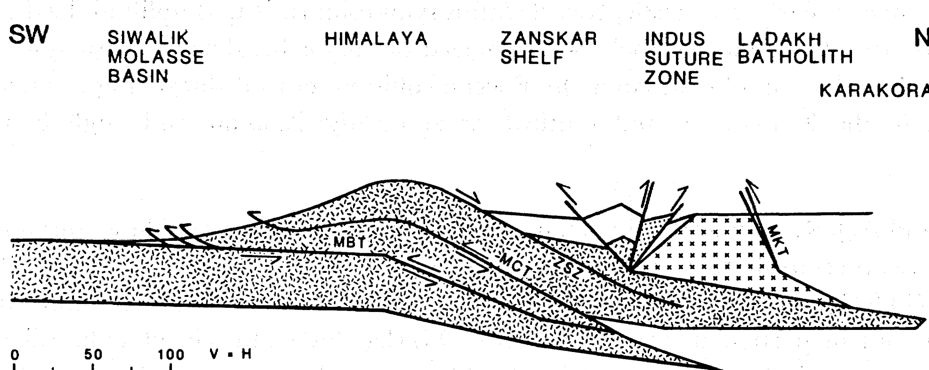

FIGURE 20. Crustal section of the western Himalaya based on Molnar (1984) but also showing the Zanskar shelf structure and ISZ from this work. See text for discussion. See Rex *et al.* (this symposium, figure 12) for a crustal section of the central Karakoram north of Ladakh.

approximately 35 km below the Indo-Gangetic Plains, and about 70 km below the Karakoram and southern Tibet (Molnar & Chen 1982). Fault-plane solutions and earthquake focal depths (Seeber *et al.* 1981) show that the Indian Plate underthrusts the Lesser Himalaya along the MBT as a coherent slab. Lyon-Caen & Molnar (1983) demonstrate from gravity anomalies in the Everest region that the dip of the Moho steepens to about 15° beneath the High Himalaya.

Molnar (1984) assumed a minimum 125 km underthrusting of Indian crust along the MCT system and a further 125 km along the MBT and Lesser Himalayan thrust systems, in central Nepal where both zones are narrower than in the western sector. In our model for the crustal structure of the West Himalaya (figure 20) we assume the MCT Zone descends to the base of the continental crust, and the minimum shortening in the High Himalayan Zone to be 200 km. Thrusting propagated southwards and the minimum amount of shortening along the MBT and Lesser Himalaya thrust sheets is likewise assumed to be 200 km. During this time, the MCT Zone was relatively inactive and being carried piggy-back by the MBT. The High Himalaya was undergoing rapid uplift by underplating beneath its southern margins, and rapid exhumation–erosion facilitated by gravitational collapse normal faulting. *P–T* estimates from metamorphic rocks of the High Himalaya southwest of the Zanskar Valley indicate that as much as 25–30 km of erosion has occurred during the last 20 Ma along the footwall of the ZSZ.

The 550 km of total shortening across the western Himalaya of India has, in our model, been taken up by crustal stacking in the Himalaya, and by underthrusting Indian crust northwards beneath the Ladakh Range north of the ISZ, and beneath the southern part of the Karakoram (bounded by the dextral Karakoram strike-slip fault that shows *ca.* 150 km of right lateral motion), but not beneath Tibet (see Rex *et al.*, this symposium, figure 12). Gravity data from the Karakoram suggest that the thickened crust is being pulled down by cold (Indian crust) material beneath it, and that the deep structure is different from that of Tibet (Molnar, this symposium).

Geological constraints from the Karakoram (Searle *et al.* 1988; Rex *et al.*, this symposium) and Tibet (Allègre *et al.* 1984) show that both have been emergent land masses since the mid-Cretaceous. England & Searle (1986) suggested that the Lhasa Block was an Andean-type margin, both in magma type and elevation (and therefore crustal thickness), before the Eocene collision. The main phase of crustal thickening and metamorphism in the Baltoro Karakoram occurred between 50–36 Ma, and resulted in intrusion of numerous syn- and post-collisional granite intrusions (Searle *et al.* 1988; Rex *et al.* this symposium). Rapid uplift and exhumation of these mid-crustal Karakoram rocks was achieved on major breakback thrust systems such as the Main Karakoram Thrust. After the Eocene collision, crustal thickening occurred both northwards in the Karakoram and southwards across the Zanskar and High Himalayan Ranges.

M. P. S. and A. J. R. both gratefully acknowledge NERC postdoctoral fellowships and grant GR3/4242 awarded to Brian Windley. D. J. W. C. gratefully acknowledges NERC fellowship and grant GTS/F/85/GS4. We thank all our Ladakhi, Zanskari and Kashmiri trekking companions and in particular Sonam Targis of Marka, Fida Hussein of Leh, Ali Hussein Shillikchey of Kargil, John Mohammed Shalla of houseboat Rolex and the lamas of Rangdum and Phugtal gompas. Sue Button is thanked for excellent cartographic work.

References

Allègre, C. J. *et al.* 1984 *Nature, Lond.* **307**, 17–22.

Andrieux, J., Arthaud, F., Brunel, M. & Sauniac, S. 1981 *Bull. Soc. géol. Fr.* **23**, 651–661.

Bard, J. P. 1983 *Earth planet. Sci. Lett.* **65**, 133–144.

Bassoullet, J.-P., Colchen, M., Guex, J., Lys, M., Marcoux, J. & Mascle, G. 1978 *C.r. hebd. Séanc. Acad. Sci., Paris* **287**, 677–678.

Bassoullet, J.-P., Colchen, M., Marcoux, J. & Mascle, G. 1981 *Riv. ital. Paleont. Stratigr.* **86**, 825–844.

Baud, A., Arn, B., Bugnon, P., Crisinel, A., Dolivo, E., Escher, A., Hammerschlag, J. G., Marthaler, M., Masson, H., Steck, A. & Tieche, J.-C. 1982 *Bull. Soc. géol. Fr.* **24**, 341–361.

Baud, A., Gaetani, M., Garzanti, E., Fois, E., Nicora, A. & Tintori, A. 1984 *Eclog. geol Helv.* **77**, 171–197.

Brookfield, M. E. & Westermann, G. E. G. 1982 *J. geol. Soc. India* **23**, 263–266.

Brookfield, M. E. & Andrews-Speed, C. P. 1984*a* *Sediment. Geol.* **40**, 249–286.

Brookfield, M. E. & Andrews-Speed, C. P. 1984*b* *Geol. Rdsch.* **73**, 175–193.

Brunel, M. 1986 *Tectonics* **5**, 247–265.

Burchfield, C. & Royden, L. 1985 *Geology* **13**, 679–682.

Burg, J.-P. & Chen, G. M. 1984 *Nature, Lond.* **331**, 219–233.

Burg, J.-P., Brunel, M., Gapais, D., Chen, G. M. & Liu, G. H. 1984 *J. struct. Geol.* **6**, 535–542.

Butler, R. W. H. 1986 *J. geol. Soc. Lond.* **143**, 857–873.

Butler, R. W. H. 1987 *J. geol. Soc. Lond.* **144**, 619–634.

Caby, R., Pêcher, A. & Le Fort, P. 1983 *Revue Géogr. phys. Géol. dyn.* **24**, 89–100.

Colchen, M. & Reuber, I. 1986 *C.r. Rebd. Séanc. Acad. Sci., Paris* **303**, 719–724.

Colchen, M., Mascle, G. & Van Haver, T. 1986 In *Collision tectonics* (ed. M. P. Coward & A. C. Ries), pp. 173–184. Geol. Soc. Lond. Spec. Publ. no. 19. London: Blackwell.

Colchen, M., Reuber, I., Bassoullet, J.-P., Bellier, J.-P., Blondeau, A., Lys, M. & De Wever, P. 1987 *C.r. hebd. Séanc. Acad. Sci., Paris* **305**, 403–406.

Coleman, R. G. 1971 *J. geophys. Res.* **76**, 1212–1222.

Coward, M. P. & Butler, R. H. W. 1985 *Geology* **13**, 417–420.

Coward, M. P., Windley, B. F., Broughton, R., Luff, I. W., Petterson, M. G., Pudsey, C., Rex, D. & Khan, M. A. 1986 In *Collision Tectonics* (ed. M. P. Coward & A. C. Ries), pp. 203–219. Geol. Soc. Lond. Spec. Publ. no. 19. London: Blackwell.

Deniel, C. 1985 Ph.D. thesis, University of Clermont.

Dietrich, V. J., Frank, W. & Honegger, K. 1983 *J. Volc. Geotherm. Res.* **18**, 405–433.

England, P. C. & Searle, M. P. 1986 *Tectonics* **5**, 1–14.

Ferrara, G., Lombardo, B., Tonarini, S. & Turi, B. 1986 Abstract, Himalayan workshop, Nancy.

Frank, W., Gansser, A. & Trommsdorff, V. 1977 *Schweiz. miner. petrogr. Mitt.* **57**, 89–113.

Fuchs, G. 1977 *Jb. geol.* B.-A **120**, 219–229.

Fuchs, G. 1979 *Jb. geol.* B.-A **122**, 513–540.

Fuchs, G. 1982 *Jb. geol.* B.-A **125**, 1–50.

Gaetani, M., Nicora, A. & Premoli Silva, I. 1980 *Riv. ital. Paleont. Stratigr.* **86**, 127–166.

Gaetani, M., Nicora, A., Premoli Silva, I., Fois, E., Garzanti, E. & Tintori, A. 1983 *Riv. ital. Paleont. Stratigr.* **89**, 81–118.

Gaetani, M., Casnedi, R., Fois, E., Garzanti, E., Jadoul, F., Nicora, A. & Tintori, A. 1986 *Riv. ital. Paleont. Stratigr.* **91**, 443–478.

Gansser, A. 1964 *Geology of the Himalayas.* 289 pages. London: J. Wiley.

Gansser, A. 1977 *Sci. Terre Himalaya: C.N.R.S.* **268**, 147–166.

Garzanti, E., Casnedi, R. & Jadoul, F. 1986 *Sediment. Geol.* **42**, 237–265.

Gilbert, E. & Merle, O. 1987 *J. struct. Geol.* **9**, 481–490.

Gupta, V. J. & Kumar, S. 1975 *Geol. Rdsch.* **64**, 540–563.

Herren, E. 1987 *Geology* **15**, 409–413.

Heim, A. & Gansser, A. 1939 *Denkschr. schweiz. naturf. Ges.* **73**, 1–245.

Hollister, L. F. & Crawford, M. C. 1986 *Geology* **14**, 558–561.

Honegger, K. 1983 Ph.D. thesis, ETH Zürich.

Honegger, K., Dietrich, V., Frank, W., Gansser, A., Thoni, M. & Trommsdorff, V. 1982 *Earth planet. Sci. Lett.* **60**, 253–292.

Honegger, K. & Raz, U. 1985 Abstract, Himalayan workshop, Leicester.

Honegger, K., Le Fort, P. & Mascle, G. 1985 Abstract, Himalayan workshop, Leicester.

Jadoul, F., Fois, E., Tintori, A. & Garzanti, E. 1985 *Rc. Soc. geol. ital.* **8**, 9–13.

Jan, M. Q. 1985 *Geol. Bull. Peshawar Univ.* **18**, 1–40.

Jaupart, C. & Provost, A. 1985 *Earth planet. Sci. Lett.* **73**, 385–397.

Johnson, B. D., Powell, C. McA. & Veevers, J. J. 1976 *Bull. geol. Soc. Am.* **87**, 1560–1566.

Kelemen, P. B. & Sonnenfeld, M. D. 1983 *Schweiz. miner. petrogr. Mitt.* **63**, 267–287.

Kelemen, P. B., Reuber, I. & Fuchs, G. 1988 *J. struct. Geol.* **10**, 129, 130.

Klootwijk, C. J. 1979 In *Structural geology of the Himalaya* (ed. P. S. Saklini), pp. 307–360. New Delhi: Today and Tomorrow Publishers.
Klootwijk, C. J. & Radhakrishnamurthy, C. 1981 In *Palaeo-reconstruction of the continents*. Geodynamic Series no. 2, pp. 93–105.
Kundig, R. 1989 *J. metamorph. Geol.* (In the press.)
Le Fort, P. 1975 *Am. J. Sci.* **275** A, 1–44.
Le Fort, P., Debon, F., Pêcher, A., Sonet, J. & Vidal, P. 1986 *Sci. Terre, Mem.* **47**, 191–209.
Le Fort, P., Cuney, M., Deniel, C., France-Lanord, C., Sheppard, S. M. F., Upreti, B. N. & Vidal, P. 1987 *Tectonophysics* **134**, 39–57.
Lydekker, R. 1883 *Mem. geol. Surv. India* **22**, 108–122.
Lyon-Caen, H. & Molnar, P. 1983 *J. geophys. Res.* **88**, 8171–8192.
Maluski, H. & Matte, P. 1984 *Tectonics* **3**, 1–18.
Mattauer, M. 1986 In *Collision tectonics* (ed. M. P. Coward & A. C. Ries), *Geol. Soc. Lond. Spec. Publ. no.* **19**, pp. 37–50.
McKenzie, D. P. 1969 *Geophys. Jl R. astr. Soc.* **18**, 1–69.
Molnar, P. 1984 *A. Rev. Earth planet. Sci.* **12**, 489–518.
Molnar, P. & Tapponnier, P. 1975 *Science, Wash.* **189**, 419–426.
Molnar, P. & Gray, D. 1979 *Geology* **7**, 58–62.
Molnar, P. & Chen, W. P. 1982 In *Mountain building processes* (ed. U. Breigel & K. Hsu), pp. 41–57. New York: Academic Press.
Nanda, M. M. & Singh, M. P. 1977 *Himalayan Geol.* **6**, 364–388.
Patriat, P. & Achache, J. 1984 *Nature, Lond.* **311**, 615–621.
Pearce, J. A. & Cann, J. R. 1973 *Earth planet. Sci. Lett.* **19**, 290–300.
Pêcher, A. 1975 *Himalayan Geol.* **5**, 115–132.
Pêcher, A. 1977 *Colloques int. Cent. natn. Rech. scient.* **268**, 301–318.
Petterson, M. G. & Windley, B. F. 1985 *Earth planet. Sci. Lett.* **74**, 45–57.
Pickering, K. T., Searle, M. P. & Cooper, D. J. W. 1987 Abstract, Himalayan workshop, Nancy.
Pierce, W. J. 1978 *Geophys. Jl R. astr. Soc.* **52**, 277–311.
Pinet, C. & Jaupart, C. 1987 *Earth planet. Sci. Lett.* **84**, 87–99.
Pognante, U., Genovese, G., Lombardo, B. & Rossetti, P. 1987 *Rc. Soc. miner. petr. ital.* **42**, 95–102.
Powell, C. McA. & Conaghan, P. J. 1973 *J. Geol.* **81**, 127–143.
Pudsey, C. J. 1986 *Geol. Mag.* **123**, 405–423.
Radhakrishna, T., Rao, V. D. & Murali, A. V. 1984 *Tectonophysics* **108**, 135–153.
Reuber, I. 1986 *Nature, Lond.* **321**, 592–596.
Reuber, I., Montigny, R., Thuizat, R. & Heitz, A. 1987 Abstract, Himalayan workshop, London.
Richardson, S. W. & England, P. C. 1979 *Earth planet. Sci. Lett.* **42**, 183–190.
Schärer, U. & Allègre, C. J. 1982 *Nature, Lond.* **295**, 585–587.
Schärer, U., Hamet, J. & Allegre, C. J. 1984 *Earth planet. Sci. Lett.* **67**, 327–339.
Schärer, U. 1984 *Earth planet. Sci. Lett.* **67**, 191–204.
Schärer, U., Xu, R. H. & Allègre, C. J. 1986 *Earth planet. Sci. Lett.* **77**, 35–48.
Sclater, J. G. & Fischer, R. L. 1974 *Bull. geol. Soc. Am.* **85**, 683–702.
Searle, M. P. 1983 *Trans. R. Soc. Edinb.* **73**, 205–219.
Searle, M. P. 1985 *J. struct. Geol.* **7**, 129–144.
Searle, M. P. 1986 *J. struct. Geol.* **8**, 923–936.
Searle, M. P. 1988 *J. struct. Geol.* **10**, 130–132.
Searle, M. P. & Fryer, B. J. 1986 In *Collision tectonics* (ed. M. P. Coward & A. C. Ries), *Geol. Soc. Lond. Spec. Publ. no.* 19, pp. 185–201. London: Blackwell.
Searle, M. P., Rex, A. J., Tirrul, R., Rex, D. C. & Barnicoat, A. 1988 *Bull. geol. Soc. Am.* (In the press.)
Searle, M. P. & Stevens, R. K. 1984 In *Ophiolites and oceanic lithosphere* (ed. I. G. Gass, S. J. Lippard & A. W. Shelton), *Geol. Soc. Lond. Spec. Publ. no.* 13, pp. 185–201. London: Blackwell.
Searle, M. P., Windley, B. F., Coward, M. P., Cooper, D. J. W., Rex, A. J., Li Tingdong, Xiao Xuchang, Jan, M. Q., Thakur, V. C. & Kumar, S. 1987 *Bull. geol. Soc. Am.* **98**, 687–701.
Seeber, L., Armbruster, J. & Quittmeyer, R. C. 1981 In *Zagros, Hindu Kush, Himalaya, geodynamic evolution* (ed. H. K. Gupta & F. M. Delany), Geodynamics Series no. 3, pp. 215–242. Washington, D.C.: American Geophysics Union.
Shah, S. K., Sharma, M. L., Gergan, J. T. & Tara, C. S. 1976 *Himalayan Geol.* **6**, 534–556.
Shams, F. A. 1980 *Geol. Bull. Peshawar Univ.* **13**, 67–70.
Shams, F. A., Jones, G. C. & Kempe, R. D. C. 1980 *Mineralog. Mag.* **43**, 941–942.
Sharma, K. K. & Kumar, S. 1978 *Himalayan Geol.* **8**, 252–287.
Sinha-Roy, S. 1982 *Tectonophysics* **84**, 197–224.
Srimal, N., Basu, A. R. & Kyser, R. K. 1987 *Tectonics* **6**, 261–274.
Staubli, A. 1989 *J. metamorph. Geol.* (In the press.)
Tahirkheli, R. A. K. & Jan, M. Q. 1979 *Geol. Bull. Peshawar Univ.* Spec. Issue II, pp. 1–30.
Tapponnier, P. *et al.* 1981 *Nature, Lond.* **294**, 405–410.

Tewari, B. S. & Sharma, S. P. 1972 *Bull. Indian geol. Ass.* **5**, 52–62.
Thakur, V. C. 1981 *Trans. R. Soc. Edinb.* **72**, 890–897.
Thakur, V. C. 1987 *Tectonophysics* **134**, 91–102.
Van Haver, T. 1984 Ph.D. thesis. Grenoble.
Wadia, D. N. 1937 *Rec. geol. Surv. India* **72**, 151–161.
Virdi, N. S., Thakur, V. C. & Kumar, S. 1977 *Himalayan Geol.* **7**, 479–482.
Valdiya, K. 1980 *Tectonophysics* **66**, 323–348.

Discussion

EVELINE HERREN (ETH-Zentrum, Zürich, Switzerland). Field investigations in the Zanskar region made over the past 5 years indicate that there are no large-scale overthrusts present as indicated on the cross section drawn and presented by Dr Searle. For example, between the anticlinal harmonic and polyharmonic folds located east of Zosar (between Tongde and Zangla in the Zanskar region) developed in the Lilang group and the overlying Kioto limestones, no evidence has been found that indicated that thrust planes cut the folds (as shown by Dr Searle in his spoken presentation and illustrated by him in his 1986 paper). Local thrusts occur only at the base of the Permian Panjal Trap and appear to be best explained as the effect of different deformation styles dependant of the competence contrasts of the different lithologies (Herren 1987).

Careful and detailed mapping and field investigations of more than one third of the High Himalayan crystallines shown on Dr Searle's map indicate that volumetrically there are fewer Himalayan age leucogranites present than he suggests (Honegger *et al.* 1982; Honegger 1983; Herren 1987; Kündig 1989; Stäubli 1989). The amount of leucogranites in the Zanskar–Suru–Kashmir–Kishtwar area is very small compared with the great granite bodies of the eastern part of the Himalayas and these leucogranites are limited to the Haptal Tokpo Valley (Herren 1987) and to the Gumburanjon leucogranite in the Tsarap Lingti Chu Valley (Srikantia *et al.* 1978; Pognante *et al.* 1987).

References

Herren, E. 1987 Ph.D. thesis, E.T.H. Zürich.
Srikantia, S. V., Ganesan, T. M., Rao, P. N., Sinha, P. K. & Tirkey, B. 1978 *Himalayan Geol.* **8**, 1009–1033.

M. P. SEARLE AND A. J. REX. Less than one tenth of the High Himalayan area in figure 17 has been mapped in detail. There are no accurate radiometric dates on any granites from this region yet, only preliminary Miocene Rb–Sr dates by Searle & Fryer (1986) and Pognante *et al.* (1987). It is therefore not possible, without extensive geochronological studies, to state what proportion of granites are of Himalayan age. However, within the high-grade metamorphic terrane SW of the Zanskar Valley, there is a high density of two-mica, garnet and tourmaline-bearing granite, leucogranite and adamellite, with some intrusions, such as the White Sail–Papsura peaks in east Kulu, being of similar proportions to the better known Manaslu or Gangotri plutons. The fact that many of the Zanskar granites are restricted to the sillimanite and kyanite zones of Himalayan metamorphism, are spatially related to migmatites of Himalayan age, and contain mineralogy, geochemistry, O and Sr isotopic compositions compatible with the Himalayan leucogranites to the east, suggest to us that their age is also Himalayan. Heterogeneities in the composition, fluid content, and heat-production potential of the source can all produce a variety of crustally derived granites, not necessarily solely of leucogranitic variety. We do not, however, state that all the granites marked on our map are Himalayan; indeed we do not specify age simply because reliable radiometric data have yet to be obtained.

M. Colchen (*UFR Sciences, Poitiers, France*).

1. Dr Searle reports an unconformity below the Lower Eocene sediments, which in his opinion belongs to the T1 thrusts, and in his model accompanies a thrust sheet of Lamayuru sediments. In fact, the slates he reports as the Lamayuru Formation resemble those of Trias-Jurassic age in the north of the Shillakong Range, but are of Cretaceous age here. Furthermore, they are concordantly overlying the Upper Cretaceous Fatu La Formation of the Shillakong Range, and thus are not overthrusted (Colchen *et al.* 1986, 1987). This fact set right, the Eocene limestone is conformably overlying those Upper Cretaceous slates; this does not exclude numerous sedimentary gaps, but in no place does an angular unconformity give evidence of a tectonic phase.

Accordingly, no deformation on the North Indian Plate is observed before collision. Obduction itself must have occurred after the Lower Eocene, as the Spongtang ophiolite is overlying mélange series containing Limestone layers and radiolarian chert of Lower Eocene age overlying serpentinized harzburgites (Colchen *et al.* 1987; Reuber *et al.* 1988). The whole is thrusted over the nummulitic limestone discussed above. We think that this is enough evidence for obduction being post Lower Eocene and coeval to collision, a process taking a long time, between 50 Ma (initial collision) and 36 Ma, when India resumes a stable Northward drift (Achache & Patriat 1984, numerous communications this meeting).

2. My second remark concerns the deformation of the Zanskar series: I do not agree with three phases of deformation. As demonstrated above, there is no evidence of a T1 deformation before collision on the North Indian Plate.

There is a syncollisional south-vergent emplacement of ophiolite and ophiolitic mélange that, however, is not accompanied by any penetrative deformation in the substratum. The penetrative schistosity is concordant in the mélange and in the underlying cretaceous slates (Reuber *et al.* 1988). The only deformation we observe is one continuous schistose deformation of the Zanskar series resulting in folds of varying vergence from one area to the adjacent one. South-vergent folds SE of Photaksar become vertical between Yapola and south of Bodkharbu and turnover towards the north and northwest in Wakka Chu and Mulbeck Chu (Colchen & Reuber 1988). This deformation post-dates the collisional period.

A corollary is that the vergence of folds is not significant of a deformation phase and neither is cylindrical folding along an orogen.

M. P. Searle and D. J. W. Cooper. The controversy over the timing of obduction of the Spontang ophiolite has recently been discussed (see Kelemen *et al.* 1988; Searle 1988) and we do not wish to repeat these points here. We disagree with Dr Colchen that the present Spontang ophiolite and mélange sole thrust is a primary emplacement feature, as the amount of shortening in the Lower Eocene limestones is considerably less than the shortening in the Mesozoic shelf sequence. Fold axial planes and cleavage in the Kangi-la Formation slates are truncated at the unconformity and are not conformable around Lingshet although further inboard (SW) they are.

We do not base our deformation phases on differing fold facing (not vergence) directions as implied by Dr Colchen. We base them on cross-cutting thrust and fold relations and sequential restoration of balanced cross sections. The Photoksar thrust is the largest and most impressive such feature and clearly truncates earlier folds and thrusts along its footwall. Although we compartmentalize fold and thrust events, we fully recognize that the post-collision orogenic process represents a continuum.

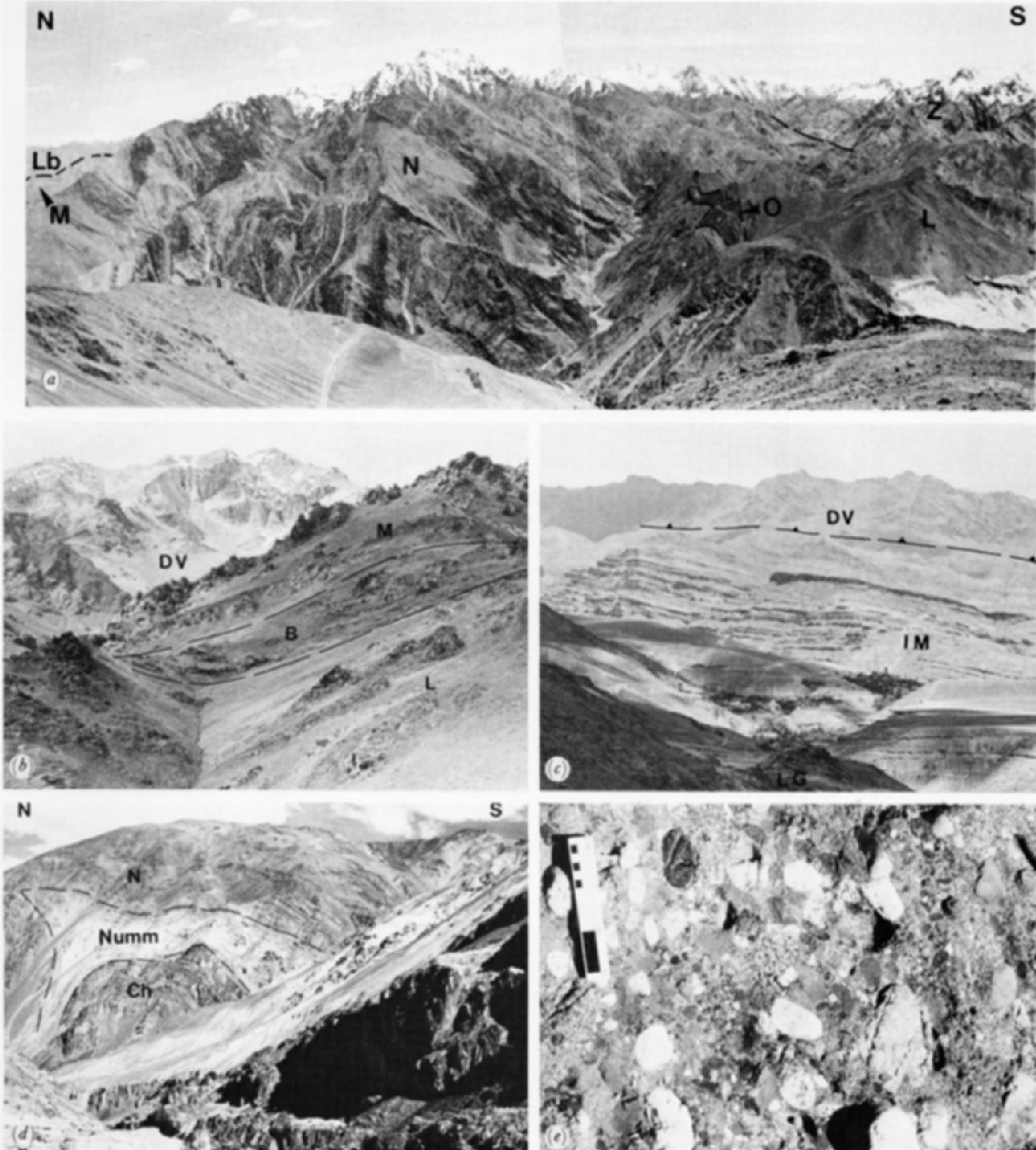

FIGURE 7. (*a*) Panorama across the Indus Suture Zone from above the Lamayuru gompa. Z, Zanskar shelf; L, Lamayuru complex; O, ophiolitic mélange; N, Nimdam Formation; M, Indus molasse; Lb, Ladakh batholith. All units dip towards S and are backthrust towards N. (*b*) The Shergol ophiolitic mélange with glaucophane-bearing blueschists (B), overlain by Indus molasse (M), north of Sapi-la. This belt of mélange separates the Lamayuru complex (L) from the Dras Volcanic Group (DV). (*c*) Indus molasse (IM) unconformably overlying the Ladakh batholith (LG) and overthrusted by the Dras Volcanic Group (DV) along a N-directed backthrust. North of Kargil. (*d*) Upright anticline in the Indus molasse along the Zanskar River section. The lower molasse unit, the Chogdo Formation (Ch) is overlain by the marine *Nummulitic* limestone (Numm) and the continental molasse of the Nurla Formation (N). (*e*) Conglomerates of the Hemis Formation in the Indus molasse. Light-coloured pebbles are Ladakh granites, andesites and dacites, dark pebbles are serpentinites and red cherts.

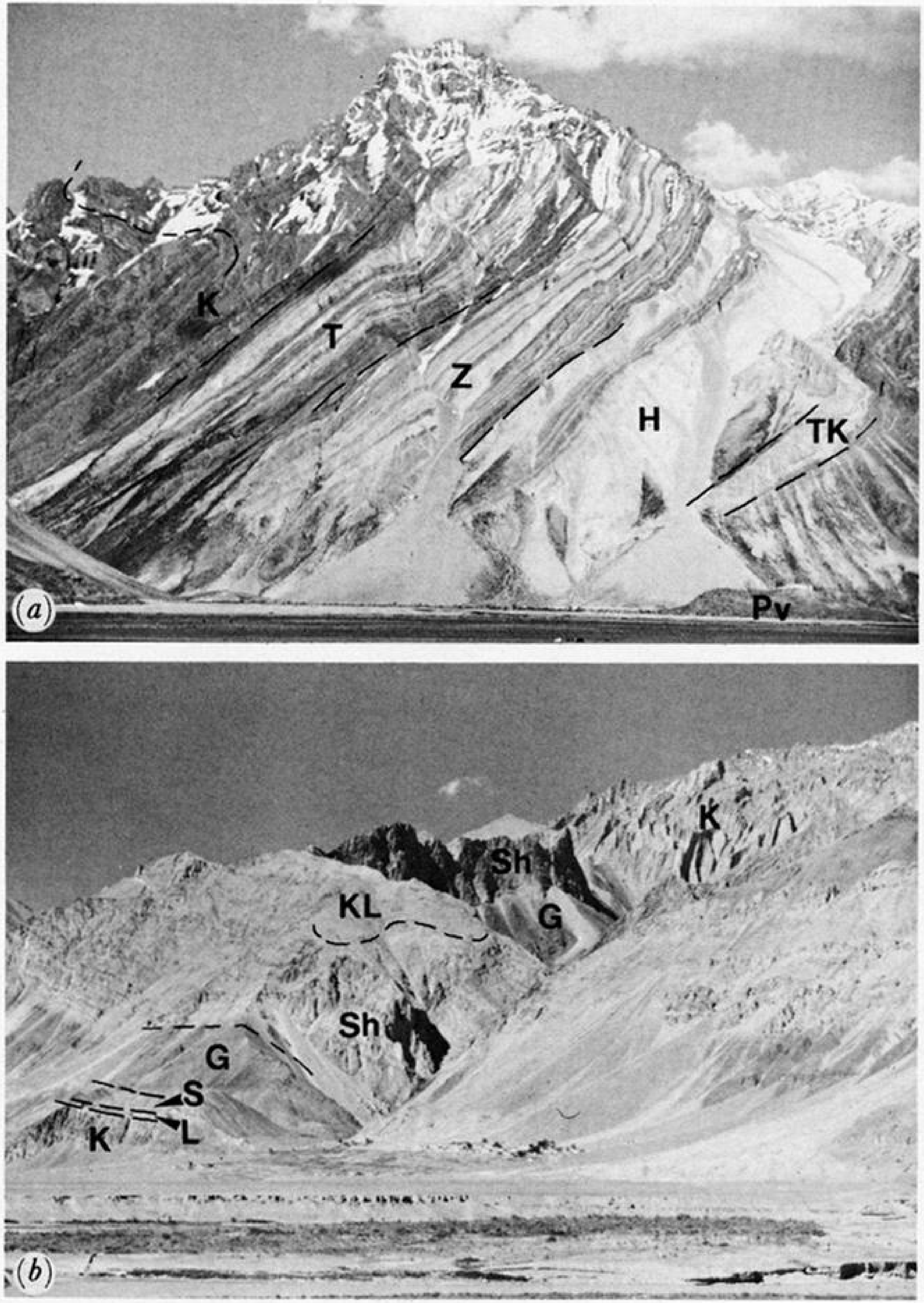

FIGURE 8. Zanskar Supergroup stratigraphy exposed at (*a*) Rangdum and (*b*) Zangla. Pv, Panjal Volcanic Group; TK, Tamba Kurkur; H, Hanse; Z, Zozar; T, Tsatsa; K, Kioto; L, Laptal; S, Spiti; G, Guimal; Sh, Shillakong; KL, Kanji-la Formations.

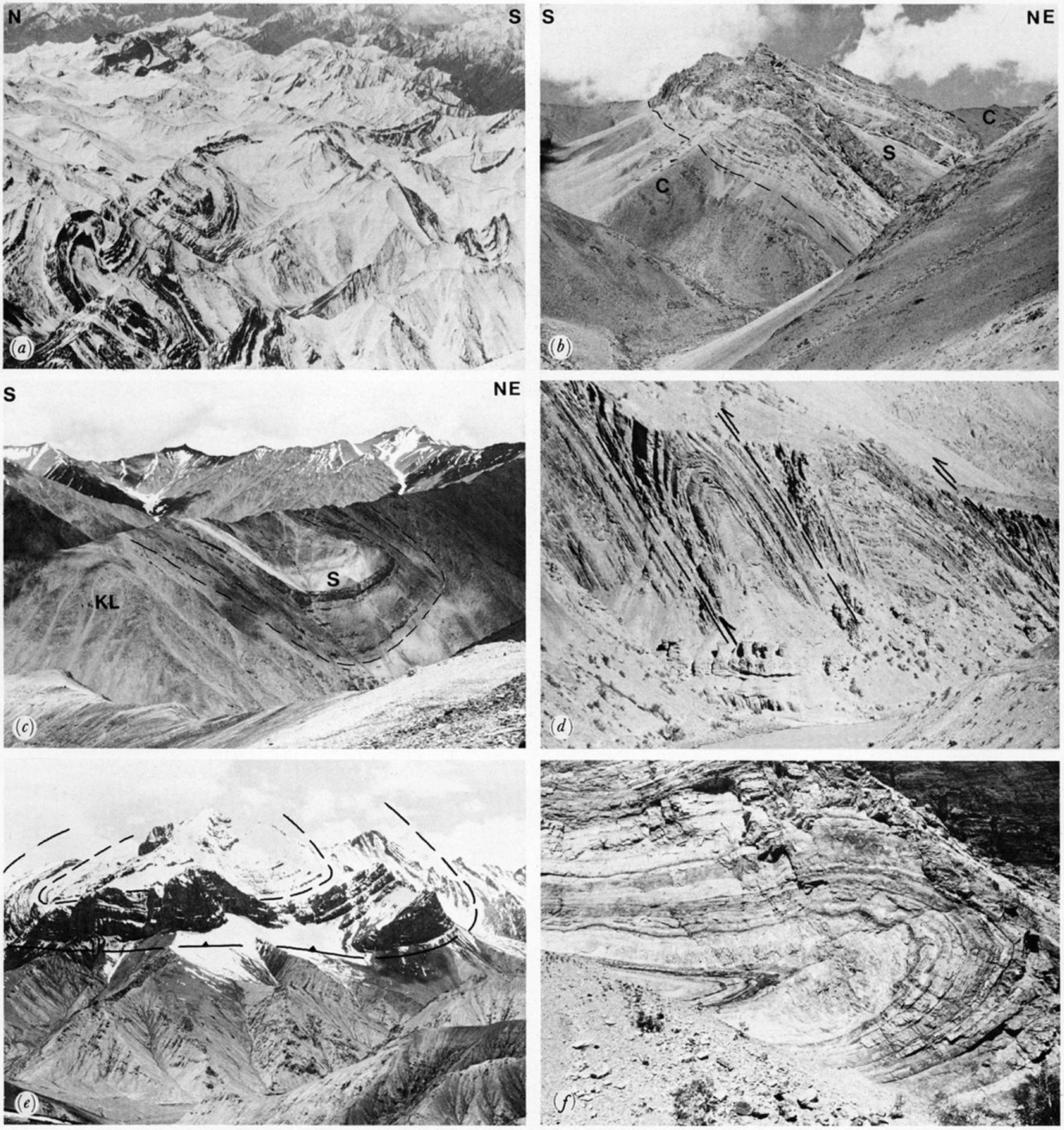

FIGURE 15. (*a*) Aerial view looking east across the northern part of the Zanskar shelf showing the northern Zanskar 'pop-up' structure with N-facing folds in the N and S facing folds in the south. (*b*) SW-facing isoclinal fold in Spanboth Formation (S) marine limestones and Chulung-la Formation (C) continental slates, N of Dibling. (*c*) SW-facing syncline in Kanji-la Formation (KL) and Spanboth Formation (S) limestones, near Kanji-la, western Zanskar. (*d*) Tight to isoclinal SW-verging folding and imbricate thrusting in Lilang group limestones, Zanskar River, N of Zangla. (*e*) Giant sheath fold in the Mesozoic shelf carbonates of the northern Zanskar unit. View S from Rubering-la, eastern Zanskar. (*f*) Isoclinal fold in Zozar Formation limestones with flat-lying axial plane, in the western Zanskar zone of lateral spreading, unnamed southern tributary of Wakka Chu, near Shergol.

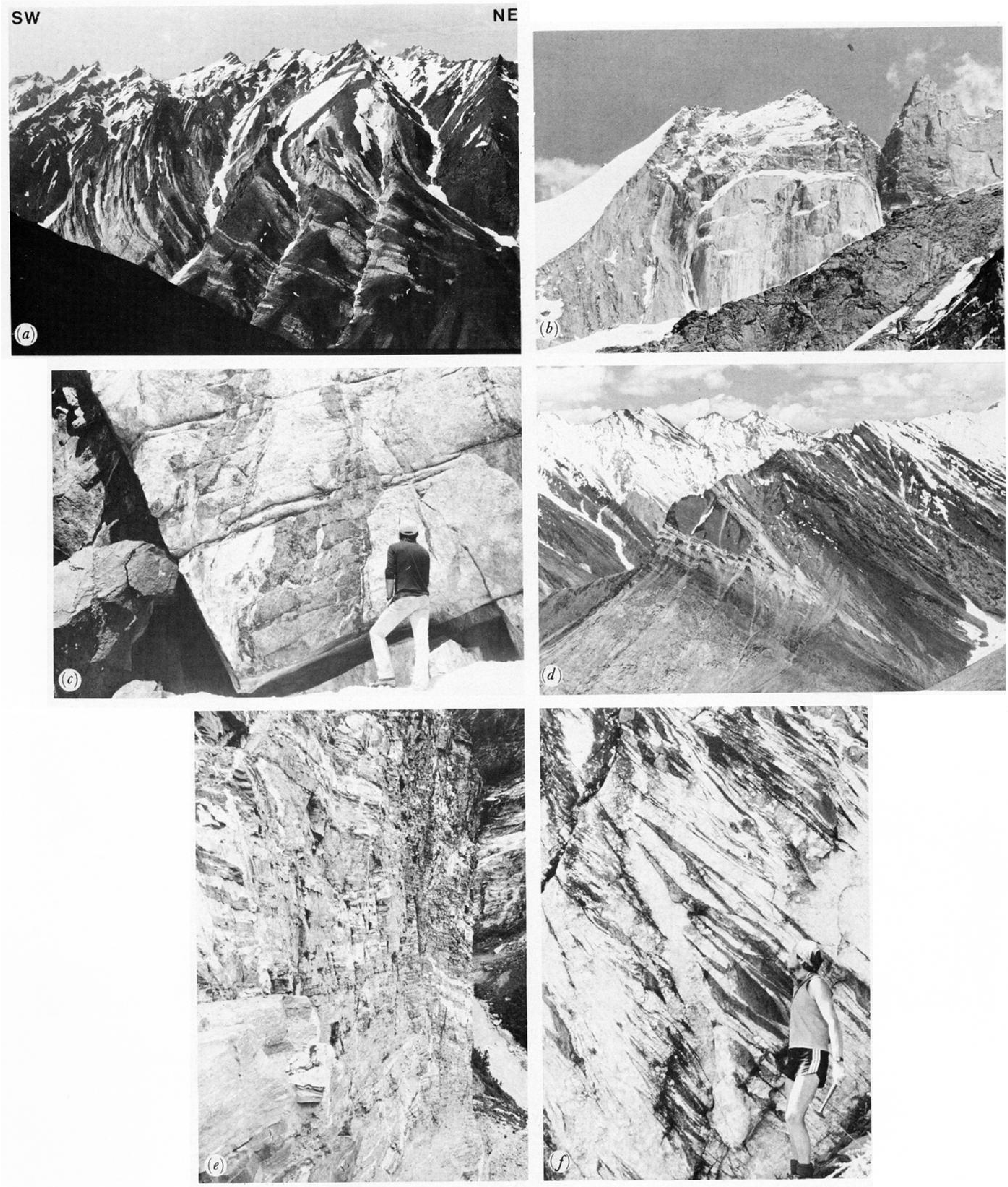

FIGURE 16. (*a*) Amphibolites, marbles and meta-pelites in a SW-verging recumbent nappe, the Donara nappe, looking N from Bobang Gali, eastern Kashmir, W of Panikar. (*b*) Upper intrusive contact of a Himalayan granite in zone 4, east of Kun. (*c*) Lower thrust contact of a sheet intrusive leucogranite in zone 3, Suru Valley near Shafat. Note ductile foliation bending into the thrust plane at base of the granite. (*d*) The Zanskar Shear Zone north of the Pensi-la showing condensed isograd sequence associated with normal faulting. (*e*) The anatectic zone 1 granite-leucogranite zone along the Chenab Valley near Dharwas. White bands are garnet–muscovite–tourmaline leucogranites, dark bands are sillimanite or kyanite-bearing gneisses. (*f*) Isoclinal folding and ductile shearing in a leucogranite mixing zone within sillimanite grade gneisses, Suru Valley.